

Modeling the Transmission Mitigation Impact of Testing for Infectious Diseases

Casey Middleton^{1,4} and Daniel B. Larremore^{1,2,3,5}

¹*Department of Computer Science, University of Colorado Boulder, Boulder, CO, USA*

²*BioFrontiers Institute, University of Colorado Boulder, Boulder, CO, USA*

³*Santa Fe Institute, Santa Fe, NM, USA*

Abstract

A fundamental question of any program focused on the testing and timely diagnosis of a communicable disease is its effectiveness in reducing community transmission. Unfortunately, direct estimation of this effectiveness is difficult in practice, elevating the value of mathematical modeling that can predict it from first principles. Here, we introduce testing effectiveness (TE), defined as the fraction by which transmission is reduced via testing and post-diagnosis isolation at the population scale, and develop a mathematical model that estimates it from the interactions of tests, within-host pathogen dynamics, and arbitrarily complex testing behaviors. While our model generalizes across pathogens, we demonstrate its flexibility through an analysis of three respiratory pathogens, influenza A, respiratory syncytial virus (RSV), and both pre-vaccine and post-vaccine era SARS-CoV-2, quantifying TE across post-exposure, post-symptom, and routine testing scenarios. We show that TE varies considerably by strategy and pathogen, with optimal testing depending on the number of tests available and when they are used. This work quantifies tradeoffs about when and how to test, providing a flexible framework to guide the use and development of current and future diagnostic tests to control transmission of infectious diseases.

To whom correspondence should be addressed: casey.middleton@colorado.edu and daniel.larremore@colorado.edu

Introduction

Nearly four years after the emergence of SARS-CoV-2, a new status quo for test usage has emerged. Despite documented successes of routine screening for SARS-CoV-2 in nursing homes [1], college campuses [2], and even nations [3], regular screening via RT-qPCR or rapid diagnostic tests (RDTs) has given way to elective testing after known exposures or symptom onset, typically with RDTs alone. At the same time, the variety and targets of available diagnostics continues to grow, with numerous available RDTs for respiratory syncytial virus (RSV; [4]) and influenza A [5], new RDTs for SARS-CoV-2 utilizing exhaled aerosols [6], and simultaneous testing for all three viruses via both multiplex RT-qPCR [7] and rapid antigen lateral flow “triple tests” [8]. Rapid diagnostics have proved valuable for non-respiratory pathogens too, including HIV [9] and *P. falciparum*, with sufficient impact for the latter that rapid diagnosis and treatment have even selected for RDT-escape mutations among *P. falciparum* parasites [10].

Mathematical models estimating the impacts of testing on transmission [2, 11–17] and treatment [18, 19] have been useful in guiding policy and recommendations for SARS-CoV-2, building in many ways on a broad set of earlier efforts to estimate transmission reduction, clinical impact, and cost effectiveness for routine HIV screening (e.g., [20, 21]). However, these successes have been restricted to a limited number of pathogens and either routine screening or risk-group based testing, highlighting the need for more flexible modeling to accommodate an increasing array of diagnostic tests for a growing set of pathogens, used after known exposures or symptom onset. Moreover, because testing guidelines are only as effective as human behaviors allow them to be, it would be valuable for models to incorporate key behaviors such as imperfect participation [9] and compliance [22] and imperfect adherence to post-diagnosis isolation [23].

Here, we fill this gap by introducing a more general mathematical model for testing without restricting our analysis to a single pathogen, test, testing pattern, or set of behaviors. Our focus was to estimate (i) the extent to which testing reduces the risk of transmission for the average infected individual, (ii) the distribution of diagnosis times and the probability that individuals are diagnosed at all, and (iii) the costs of test consumption and isolation days corresponding to these benefits. Taken together, this model places various intuitions about disease mitigation via testing on firm quantitative ground, and exposes important testing-associated variables and behaviors to *in silico* experimentation and optimization across contexts, pathogens, and variants thereof.

Results

A model for Testing Effectiveness (TE)

To examine the impact of testing on community transmission, we developed a probabilistic model which integrates four key elements: (i) the properties of a particular diagnostic test, (ii) a strategy for its administration, (iii) the time-varying profiles of infectiousness, symptoms, and detectability over the course of an infection, and (iv) the key behaviors of compliance, participation, and isolation length. Given these elements, the model generates a distribution of probable diagnosis times, and uses them to compute the expected impact on transmission. By then incorporating heterogeneity between individuals, the model estimates *testing effectiveness*,¹ the proportion by which a testing program reduces transmission, in expectation,

¹We call this quantity *testing effectiveness* instead of *test effectiveness* due to the simple observation that the same test, used differently, may have a markedly different impact.

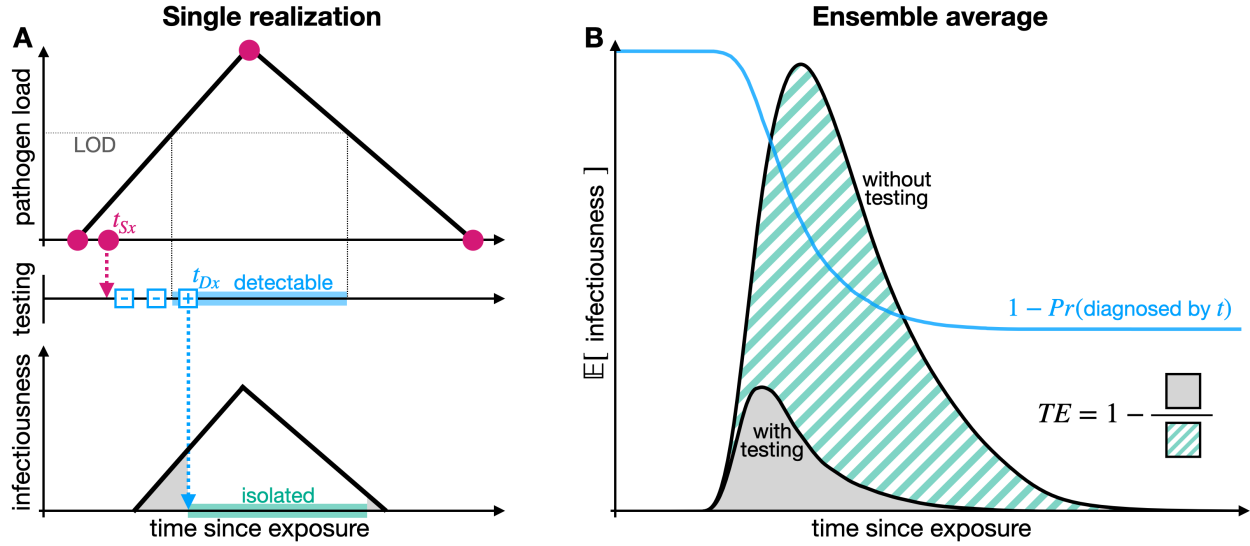


Figure 1: **Model diagram.** (A) Each realization of the stochastic testing model first draws four control points to specify a “tent function” model of pathogen load and a symptom onset time (pink circles). The realization then draws a set of testing times (blue squares), which may be triggered by symptoms (pink arrow), triggered by a known exposure (not shown), or ongoing at a particular cadence (not shown). A test taken during the detectable window (blue bar) when pathogen load exceeds the test’s limit of detection (LOD) will return a positive diagnosis with a fixed probability after a specified turnaround time (not shown). However, not all tests are necessarily taken, due to imperfect compliance (not shown). Diagnosis (Dx) leads to isolation and thus reduced infectiousness (grey). (B) The ensemble mean, whether computed through integrals or estimated via Monte Carlo, produces expected infectiousness curves with and without testing. The areas under these curves are proportional to their respective reproductive numbers, enabling estimation of testing effectiveness TE (see Eq. (1)). The model also produces an ascertainment curve (blue) showing the proportion of individuals remaining undetected at time t .

given by the relationship between reproductive numbers R with and without testing as,

$$TE = 1 - \frac{R_{\text{testing}}}{R_{\text{no testing}}} \leftrightarrow R_{\text{testing}} = (1 - TE) R_{\text{no testing}} . \quad (1)$$

We built our analyses around a simple, common, and computationally efficient model of within-host pathogen kinetics: after some post-exposure latent period, the pathogen load grows exponentially at some proliferation rate until reaching a peak, and then declines exponentially at some clearance rate. This piecewise linear model, also called a tent function, requires only the four parameters of latent, proliferation, and clearance periods, and a peak load, which we draw from distributions estimated from studies of RSV [24,25], influenza A [26–28], and SARS-CoV-2 measured for both the founder strain in naive hosts during the pre-vaccination era [12, 16, 29] and omicron variants in experienced hosts during the post-vaccination era [12, 29, 30] (see Table S1). While the results presented here utilize this simplistic model of viral kinetics, the modeling framework is highly flexible to incorporate more sophisticated alternatives.

We used stochastic realizations from this simple pathogen load model in three ways. First, we assumed that a test taken at time t would return a negative diagnosis if the pathogen load was below the test’s limit

of detection (LOD), and would return a positive diagnosis with some probability when pathogen load was above the LOD. Due to the importance of test turnaround time [12], we modeled sample-to-answer delays by returning results after a specified turn-around time (TAT). Second, we took infectiousness to be proportional to the logarithm of pathogen load in excess of an empirically estimated threshold [31, 32], consistent with observations that higher viral loads are associated with more efficient transmission for pathogens including SARS [33], SARS-CoV-2 [22], influenza [34], and RSV [35]. Alternative relationships between pathogen load and infectiousness are possible [12]. Third, we drew symptom onset times relative to the times of peak pathogen load, reflective of the typical manner of reporting in the literature. In this way, our model is similar in spirit to the CEPAC model (Cost-Effectiveness of Preventing AIDS Complications), which provides stochastic individual-level realizations of post-HIV-infection dynamics, costs, and outcomes [36].

Our model generates its estimates by integrating over the probability distributions for the pathogen load, the timing of symptoms, and the timing of tests, to calculate a distribution of diagnosis times. After receiving a diagnosis, each individual is assumed to isolate for a specified number of days, or until released by a negative test (via a so-called test-to-exit plan), with mitigated infectiousness during isolation (Fig. 1A). By averaging outcomes over the ensemble defined by its random variables, whether by integration or via Monte Carlo, the model produces estimates of the expected infectiousness curves over time, with and without testing. The areas under these two curves are proportional to the total transmission potential with and without testing, and thus, their respective reproductive numbers. The model also provides a curve representing the probability that a randomly chosen individual has not yet been diagnosed by some time; its long-time limit is the ascertainment of the testing scenario (Fig. 1B). A complete mathematical description and details of parameterizations can be found in Materials and Methods.

Testing effectiveness varies by strategy and pathogen

Despite the 2023 end to the World Health Organization's COVID-19 public health emergency [37], the burden of COVID-19 and respiratory viruses more broadly remains substantial. In the U.S. alone, an estimated 9 million cases of influenza A caused 100,000 hospitalizations (2021-2022 season; [38]), and a global estimate of 33 million RSV infections in children under 5y led to 3.6 million associated hospitalizations and 101,400 associated deaths, the vast majority of which were in low- and middle-income countries (2019; [39]). With the broad expansion of diagnostic testing globally, including at-home rapid diagnostic tests (RDTs) for influenza A, RSV, and SARS-CoV-2, we sought to determine whether a single testing strategy might be optimal for all three common respiratory pathogens.

To examine the potential impacts of testing, we considered three distinct testing behaviors, meant to capture both institutional testing strategies and elective testing in response to exposure or symptoms. First, we considered an elective testing scenario in which individuals experiencing symptoms used one rapid diagnostic test (RDT) per day for 2d following the onset of symptoms (TAT = 0; see Table S1 for stochastic timing and prevalence of symptoms). Given the markedly different sensitivities of different RDT kits and RT-qPCR protocols [40, 41], a representative LOD was chosen for each respiratory virus to investigate general principles of testing (see Materials and Methods). Second, we considered an elective testing scenario in which 75% of individuals sought out a single RT-qPCR test (TAT = 2, see Table S1 for LODs) between 2d and 7d after exposure; the other 25% did not participate. Finally, we considered routine weekly screening with a representative rapid diagnostic test (TAT = 0, LODs Table S1). To incorporate the fact that not all policy-prescribed tests are actually taken in practice [22], this scenario included compliance of only 50%, such that each test was taken or not taken independently with probability $\frac{1}{2}$. For each scenario, and each of the three circulating respiratory viruses (RSV, influenza A, and SARS-CoV-2), we calculated TE , the

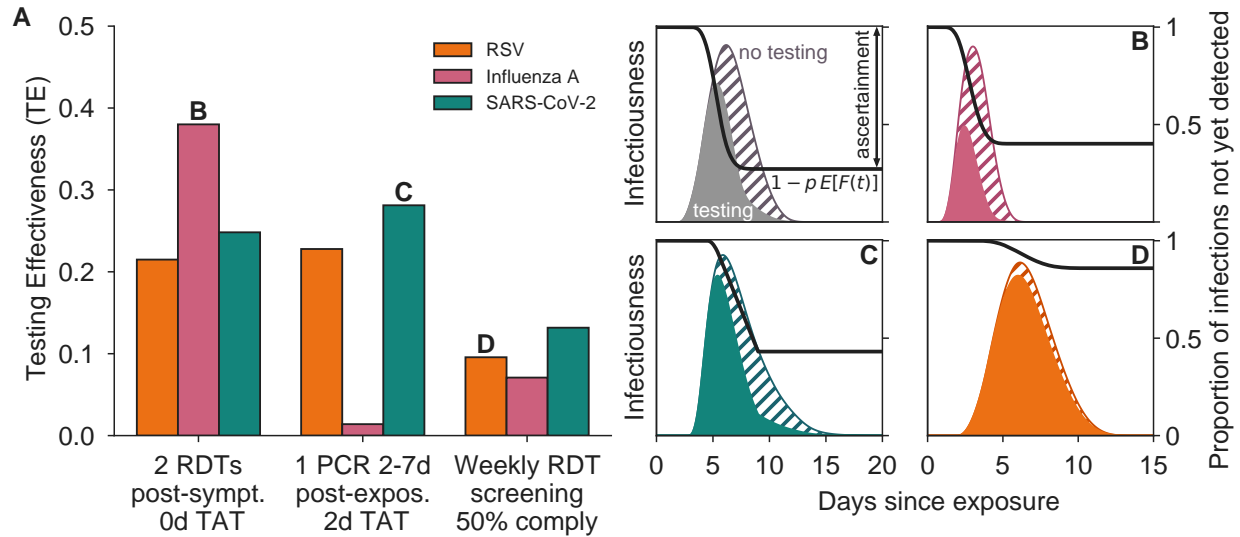


Figure 2: Testing effectiveness varies considerably by strategy and pathogen. Testing effectiveness is shown for RSV (orange), influenza A (pink), and SARS-CoV-2 omicron in experienced hosts (green) under three testing programs: (1) testing with two RDTs used daily starting at symptom onset, (2) one RT-qPCR test administered 2-7d after exposure, with 75% participation and 2d test turnaround time, (3) weekly RDT screening with 50% compliance. Panels A, B, and C depict population-level infectiousness curves without (hatched) and with (filled) testing and isolation for the labeled pathogen and testing program. Black curves represent the proportion of infections not yet detected by time t .

timing of diagnoses, and ascertainment—the total fraction of individuals receiving a positive diagnosis—based on 10^5 stochastic realizations of viral load, symptom onset, testing, diagnosis, and isolation. For SARS-CoV-2 we specifically considered within-host dynamics and RDTs associated with omicron variants in immune-experienced hosts.

This analysis demonstrated that the same testing program can have markedly different effectiveness for different pathogens. Elective testing at symptom onset achieved 38% TE for influenza A, but only 21% for RSV (Fig 2A). This difference in effectiveness primarily reflects differences in the relative timing of symptoms and detectability, with most influenza A infections detectable via RDT one day before or after symptom onset, whereas RSV is generally only detectable 1-3 days *after* symptom onset. In contrast, TE for elective testing at SARS-CoV-2 symptom onset is middling at 25%, balancing well-timed symptom onset relative to infectiousness, but a higher relative LOD for marketed RDTs. Due to their highly overlapping symptom sets, our results indicate that testing immediately after symptom onset with a single three-pathogen RDT [8] is therefore likely to mitigate transmission most for influenza A, followed by SARS-CoV-2 omicron and RSV.

This ordering of differential TE was inverted for a single elective RT-qPCR between 2d and 7d post-exposure, our second testing scenario, which was least effective for influenza A (Fig. 2A). This ordering reflects a substantially faster onset of infectiousness after exposure for influenza A (Fig. 2B), meaning that a post-exposure test that is timed effectively for SARS-CoV-2 and RSV is administered too late to control influenza A. Thus, in a scenario where an individual seeks a highly sensitive multiplex diagnostic test within one week after a known exposure to an unknown respiratory pathogen, our results indicate an impact

on transmission of 28% for SARS-CoV-2, 22% for RSV, and just 2% for influenza. Finally, weekly RDT screening with 50% compliance exhibited comparable TE for all three pathogens (7-13%), values which are lower than the two elective testing scenarios for SARS-CoV-2 and RSV, and higher for influenza A. Our results highlight the fact that variation in viral kinetics, symptom onset time, and tests' analytical sensitivities lead to markedly different impacts on transmission, used under the same testing guidance.

Throughout these experiments, we observed that ascertainment—the proportion of infections diagnosed via testing—was only weakly related to TE , showing that a testing program's information value and mitigation impact are distinct quantities. For instance, elective RDT testing post-symptoms for influenza A showed TE and ascertainment of 38% and 60%, respectively; for elective RT-qPCR testing post-exposure, TE decreased by 36pp to just 2% but ascertainment decreased by only 10pp to 50%. To illustrate the reason for this difference, we plotted the infectiousness curves $\beta(t)$ with and without testing, averaged over all 10^5 simulated individuals, as well as the curves showing the fraction of individuals remaining undiagnosed $1 - p \mathbb{E}[F(t)]$ (Fig. 2B,C,D). In instances where diagnoses typically arrive earlier, the average $\beta(t)$ (and thus the area beneath it, R_{testing}) is more substantially reduced, while the same number of diagnoses, arriving later, leave more area under the $\beta(t)$ curve. Thus, TE incorporates not just whether one is diagnosed, but also when.

Impacts of timing and availability of elective post-symptom testing

In an era of increasing elective and self-administered RDT usage, a key question is when to test and how many tests to use. We sought to answer this question by modeling the impact of changes in timing and supply of RDTs on TE for RSV, influenza A, and SARS-CoV-2 omicron in experienced hosts. In these experiments, we considered that individuals would wait 0d-5d after symptoms and then begin testing daily, with 1-6 RDTs available. For comparison, we also computed TE for a single RT-qPCR with a two-day turnaround. For each testing supply, we computed TE and identified the post-symptoms delay that maximized it, separately for each virus and testing supply scenario (Fig. 3, white stars).

This experiment showed three common patterns for RSV and influenza A. First, the most effective timing of post-symptom testing was zero days, with monotonically decreasing TE with each additional day of delay (Fig. 3A,B). Second, although using two tests was superior to using one, using more than two tests was roughly equivalent to two. And third, using just one RDT provided superior TE to a single RT-qPCR with a two-day turnaround time, highlighting the importance of RDT availability for transmission control.

In contrast, for SARS-CoV-2 omicron in experienced hosts, the number of available tests markedly shifted the optimal time at which one should begin testing, such that when only 1-2 RDTs were available, daily testing was most effective beginning 2d post-symptoms; with 3 RDTs, 1d; and with 4-6 RDTs, testing should begin immediately upon symptom onset (Fig. 3C). These results reflect a tradeoff arising from limited test supply and variability in viral load trajectories: using tests later improves the probability of diagnosis but decreases the impact per diagnosis. A large test supply alleviates this tradeoff. Furthermore, for a fixed delay before testing, using more SARS-CoV-2 RDTs was always superior, yet a single RT-qPCR on the first day of symptoms provided approximately equivalent TE to using one RDT starting on day two. Together, these results suggest a unified recommendation for the timing of post-symptom elective RT-qPCR testing, but a mixed recommendation for RDT use. A similar analysis of the impact of timing and quantity of post-exposure testing is presented in Supplementary Figure S1.

One common point surfaced by our investigations of elective post-symptomatic testing was that the existence of any asymptomatic and post-symptomatic transmission implies that $TE < 1$ for symptom-driven testing,

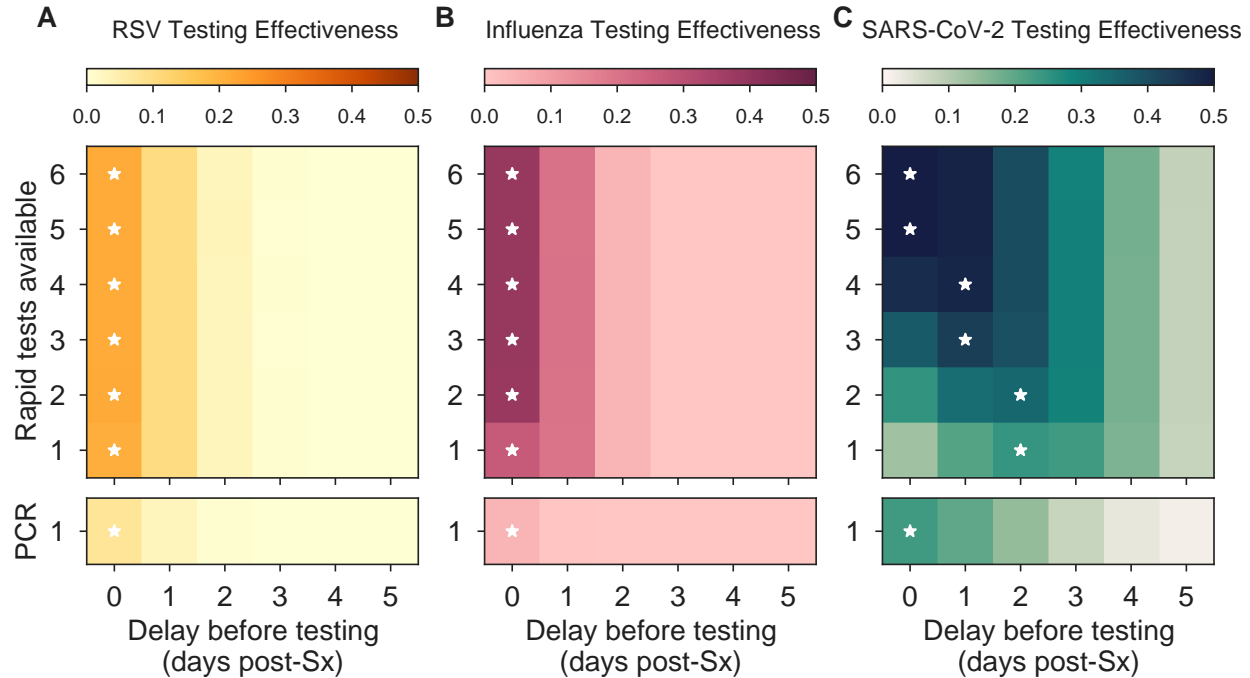


Figure 3: **Optimal use of tests depends on the number of tests available and when they are used.** Testing Effectiveness (TE) of RDT and RT-qPCR with 2 day turnaround time, used x days after symptom onset using y tests once per day is shown for RSV (orange), influenza type A (pink), and SARS-CoV-2 omicron in experienced hosts (green). Darker colors represent higher TE as indicated. In each row, the testing strategy with highest TE is annotated with a white star. Turnaround times: rapid tests, TAT = 0; RT-qPCR TAT = 2. See Supplementary Table S1 for LODs.

regardless of the quality of the diagnostic test itself. This implies that even groundbreaking advances in diagnostic LODs, cost, or turnaround times must be paired with appropriate recommendations for usage.

Reevaluation of the sensitivity/turnaround tradeoff for SARS-CoV-2

Modeling studies in 2020 and 2021 argued that test sensitivity was secondary to frequency and turnaround time for SARS-CoV-2 screening [12, 13, 42, 43], using within-host dynamics and RDT sensitivities for the founder strain in naive hosts. However, three important observations regarding the omicron variants circulating in 2023 led us to revisit these findings. First, studies of viral load trajectories, estimated via prospective longitudinal sampling, show lower peak viral loads, shorter clearance times, and slightly longer proliferation times for omicron infections in experienced hosts compared to founder-strain infections in naive hosts [16, 30], leading to shorter windows of detectability (Fig. 4A). Second, symptom onset is typically 3-5d earlier for omicron/experienced vs founder/naive, relative to peak viral load, an observation argued to be due to the immune experience of hosts in particular [30, 44, 45]. Third, the analytical sensitivity of RDTs is estimated to have worsened for omicron variants vs founder strain, with LODs increasing by 0.5 – 1.0 orders of magnitude depending on the test (Fig. 4A; [40, 41]). Together, these factors led us to hypothesize that the previously established superiority of RDTs over RT-qPCR for mitigation of founder-strain SARS-CoV-2 in a naive population could be equalized or reversed for omicron-variant SARS-CoV-2 in an experienced

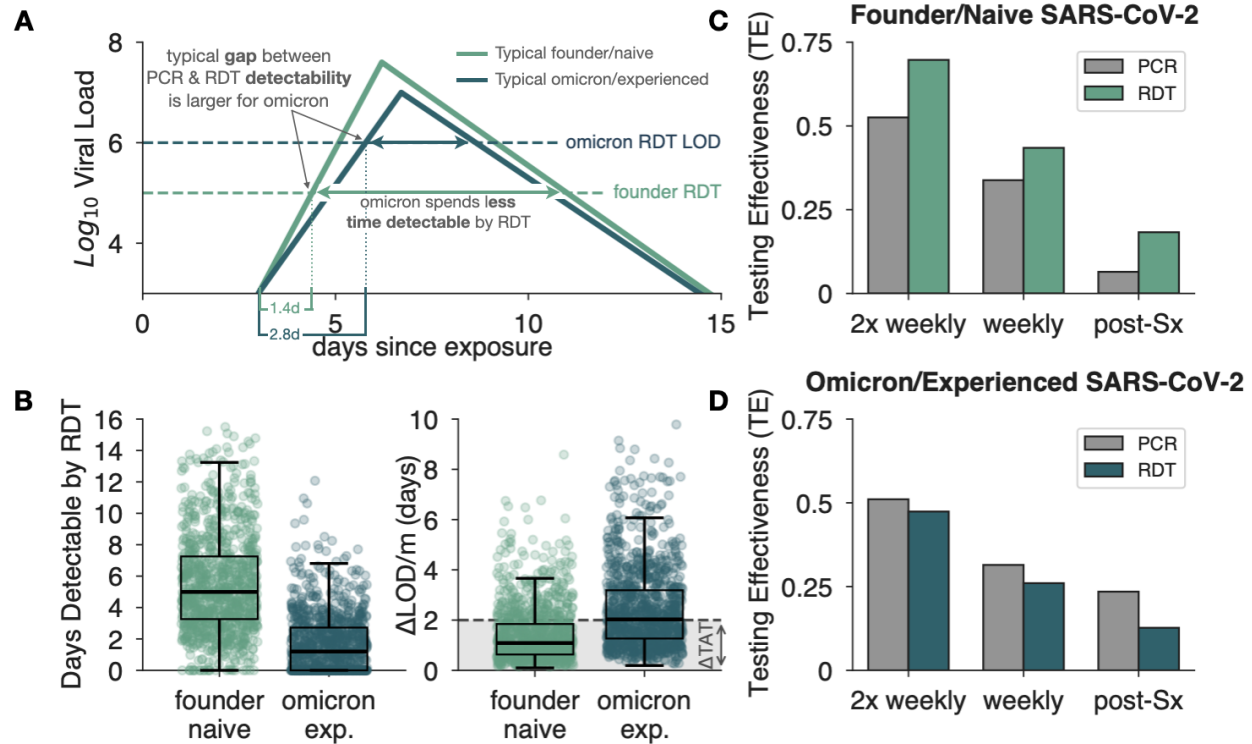


Figure 4: **RT-qPCR vs RDT tradeoffs for the SARS-CoV-2 omicron era.** (A) Typical viral kinetics for founder SARS-CoV-2 strains in naive hosts and SARS-CoV-2 omicron variants in experienced hosts (\log_{10} cp mRNA / mL). Trajectories are characterized above the RT-qPCR LOD (10^3) with their respective RDT LODs (10^5 and 10^6 for founder strain and omicron variant, respectively) indicated by horizontal dashed lines. (B) Time spent detectable by RDT and relationship between LODs of RDT and RT-qPCR vs proliferation speed for founder-strain SARS-CoV-2 in naive hosts (light) and SARS-CoV-2 omicron variants in experienced hosts (dark) scenarios. (C,D) Test effectiveness using RT-qPCR with 2 day turnaround time (gray) or RDT with immediate delivery of results (green) for twice weekly and weekly screening, or testing immediately upon symptom onset using one test.

population.

To test our hypothesis, we estimated TE for RDT testing (0d TAT) and RT-qPCR testing (2d TAT) programs, in twice-weekly, weekly, and elective post-symptom testing scenarios, and compared our findings for founder/naive vs omicron/experienced parameters. We found that in each of the three founder/naive testing scenarios, RDTs provided higher TE than RT-qPCR (Fig. 4B), replicating the claims of the literature [12,13,42,43]. However, each of the three omicron/experienced scenarios saw a reversal, with RT-qPCR providing higher TE than RDTs, despite the modeled 2d RT-qPCR turnaround time (Fig. 4C). In general, we also observed that TE decreased for RDTs from the founder-strain era to the omicron era (Fig. 4B vs C), while staying approximately the same (twice weekly, weekly) or even increasing (post-symptom) for RT-qPCR. Together, these results suggest that, setting aside any differences in cost or regulatory complexity, RT-qPCR-based SARS-CoV-2 testing would be superior to otherwise identical RDT-based testing in the omicron and immune-experienced era.

To what can we attribute this apparent reversal in the prioritization of speed vs sensitivity, and how might

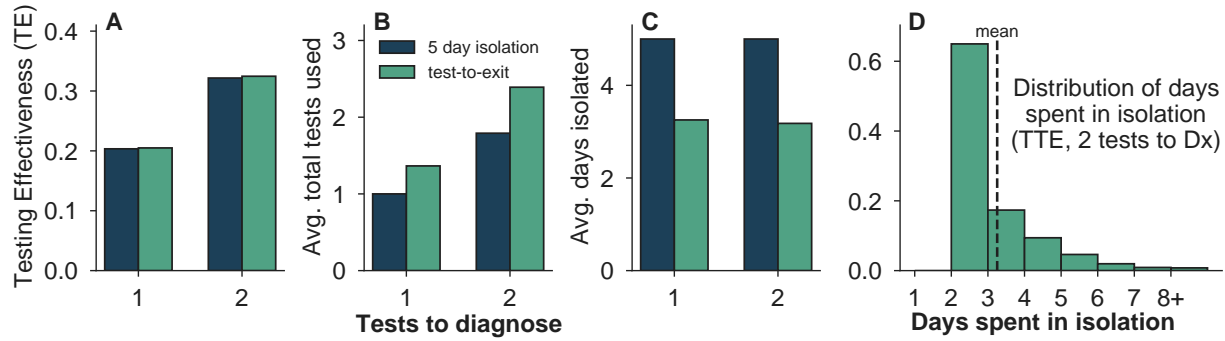


Figure 5: Fixed isolation recommendations may lead to unnecessary isolation when symptomatic testing ascertainment is high. (A) Testing Effectiveness, (B) total test consumption over diagnosis and test-to-exit usage, and (C) average isolation duration for detected individuals are shown for a fixed 5d isolation period (dark blue) and a test-to-exit isolation program requiring one negative RDT to exit isolation (light green) when 1 or 2 tests were available to diagnose, used daily beginning one day after symptom onset. (D) The distribution of individual days spent in isolation for a test-to-exit scheme using 2 tests to diagnose, with the average isolation time indicated by the vertical dashed line. TTE scenarios assumed individuals waited 2 days after diagnosis before beginning exit-testing.

such principles generalize? Intuitively, during viral proliferation, there exists a gap between the time of first detectability via RT-qPCR and the time of first detectability via RDT. This gap represents a potential diagnostic advantage for the RT-qPCR test, but it can be realized only if (i) a test is actually taken during the gap, and (ii) the turnaround time for the RT-qPCR is smaller than the gap. For founder-strain SARS-CoV-2 in the naive host, we estimate the typical gap (over diverse viral load trajectories) to be 1.4d, vs 2.8d for SARS-CoV-2 omicron variants in experienced hosts (Fig. 4A). Quantifying this intuition, we reason that when two tests exhibit a difference in LOD of Δ_{LOD} and a difference in turnaround time of Δ_{TAT} , then the faster test will typically exhibit higher TE when $\Delta_{\text{LOD}}/m + \delta_{\text{TAT}} > 0$, where m is the typical exponential proliferation rate.

Estimating costs: isolation days and test consumption

Diagnosis-driven isolation provides a mitigation benefit of TE , but at the cost of testing resources and days spent in isolation. Therefore, in addition to quantifying the benefits of TE and ascertainment, we estimated the costs of test consumption and isolation days (Materials and Methods). When calculating these costs, we also recognized that diagnostic tests may be used to determine when one should exit isolation, via so-called test-to-exit (TTE) guidelines [46], potentially increasing test consumption in order to decrease isolation days, with the additional risk of early release from isolation due to a non-analytical test failure. Based on these modeling needs, we modified our estimates of all model outputs to incorporate TTE strategies (Supplementary Text).

To explore the ways in which our model could assist in evaluating complex cost-benefit tradeoffs across scenarios, we considered elective post-symptom testing for SARS-CoV-2 omicron variants in experienced hosts, using either one or two RDTs daily after symptom onset to attempt diagnosis. Diagnosis was followed by either a fixed-duration isolation of 5d or a TTE policy of daily testing using the same RDT, beginning after a minimum of 2d spent in isolation. In each of the 2×2 scenarios, we computed TE , the average

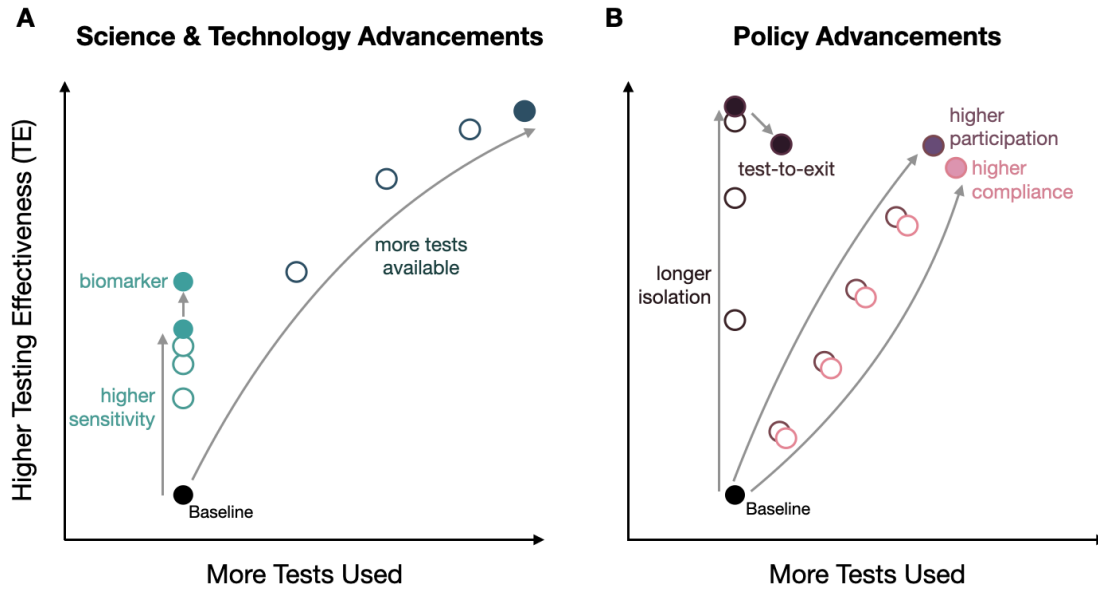


Figure 6: **Schematic of various technological and policy advances in cost-benefit space.** Increases testing effectiveness (TE) and test consumption are shown for a set of hypothetical improvements to technology, policy, and cost of goods.

number of tests consumed per infected individual, and the average number of isolation days per diagnosed individual.

At a high level, using two tests to diagnose led to substantially higher TE than using just one (Fig. 5A), mirrored by an increase in per-infection testing cost from 1 to 1.8 tests for the fixed-isolation scenario, and from 1.4 to 2.4 for the TTE scenario (Fig. 5B). Average isolation days per diagnosis were identically 5d for the two-fixed isolation scenarios by definition, and reduced to 3.2-3.3d for TTE (Fig. 5C). Thus, as intended, TTE programs decreased average isolation days without a large impact on TE , driven by the fact that the most common outcome of TTE was release after just 48-72h, while nevertheless maintaining long isolations for those remaining detectable for longer periods (Fig. 5D).

Modeling to guide R&D and policy advances

The ability to prospectively estimate costs (test consumption) and benefits (TE) for a diagnostic test, its recommended use, and individual behaviors, means that hypothetical advances in technology and policy may be explored *in silico* to evaluate the potential value of investments. For instance, we projected that a technological advance in analytical sensitivity, or the derivation of a novel biomarker enabling earlier detection, would increase TE for the same test consumption, while investments in manufacturing which decrease unit costs would make more tests available, thus increasing both consumption and TE , with decreasing marginal returns to consumption (Fig. 6A). Similarly, a policy shift encouraging additional people to participate in testing would increase both TE and test consumption, while encouragement of higher compliance among those already participating would do the same but typically with slightly higher consumption and slightly lower TE (Fig. 6B). Building on our conceptual cost-benefit diagrams, concrete cost-benefit projections for hypothetical changes to technology, policy, and behavior may be computed using this testing effectiveness

model.

Discussion

This study quantifies the impact of testing as a non-pharmaceutical intervention by defining testing effectiveness (TE) as the expected reduction in the risk of transmission for a particular testing behavior, test, and infecting pathogen. While TE varies considerably across the scenarios we explored, three general principles emerge. First, no single elective testing strategy provides superior control across respiratory viruses, due to important differences in their dynamics within host. This highlights the importance of models linking within-host kinetics to between-host transmission when establishing testing guidelines, and the risks of blanket recommendations for respiratory virus transmission control. Second, elective post-symptom or post-exposure testing can have a substantial impact on transmission, but timing is important and depends on the pathogen, test, and available supply. While greater availability of tests leads to strictly larger TE , in supply-limited scenarios, a strategic delay may lead to greater TE by diagnosing more infections, even if they are not detected as early. Last, by modeling tests and testing through different parameters, our analyses show the importance of key behaviors, including compliance, post-diagnosis isolation, and the manner in which to test. These present opportunities to markedly increase the mitigation impact of testing through not only test technology and availability, but through usage guidance and policy as well, based on quantitative guidance from the model.

This work builds on strengths of three established threads in the literature. Many high-quality studies have estimated the value of testing, particularly for routine SARS-CoV-2 screening under a variety of assumptions [2, 11, 13–15, 17, 18, 47], and for HIV [9, 20, 21, 36]. Recognizing the growing availability of test options for other pathogens [7, 8] and the collapse of regular SARS-CoV-2 screening programs in favor of elective post-symptom or post-exposure testing, our work proposes a more general framework to meet the current and future realities of testing. This work also builds on the concept of symptom-based controllability [15, 48, 49] by considering a type of diagnosis-driven controllability, and quantifying how much of the theoretical value of symptom-based control can be realized when individuals require a diagnosis before deciding to isolate. Third, this work adds TE to the set of estimates quantifying the effectiveness of targeted interventions that can be directly incorporated as single parameters in between-host transmission models, including vaccine effectiveness [50] and PrEP efficacy [?]. Conceptually, testing effectiveness may be implemented as an increased recovery rate [51] or decreased transmission probability in between-host models.

By exploring TE under various testing scenarios for three common respiratory viruses, this study demonstrated that an effective strategy for one pathogen may be ineffective for another, and vice versa. This is driven by the complex tradeoffs between a test's timing, probability of diagnosis, and number of potentially avoided future transmissions should the test come back positive. Intuitively, early testing leads to fewer diagnoses with higher impact per diagnosis, while delayed testing leads to more diagnoses but lower impact per diagnosis. Mathematical models integrating over these contingent factors, stochasticity, and heterogeneity between individual infections, are critical to putting this intuition on a quantitative foundation. Exemplifying this value, our analysis showed that testing with a slower but more sensitive RT-qPCR exhibited a higher TE than otherwise identical rapid antigen testing for SARS-CoV-2 omicron variants in experienced hosts (but not founder SARS-CoV-2 strains in naive hosts), updating a previously published finding that emphasized turnaround time over sensitivity for founder-strain SARS-CoV-2 [12].

The model introduced in this manuscript was necessary because empirical evaluation of the impact of a testing program or behavior is difficult, with compelling analyses nevertheless lacking formal controls [2,3] or requiring enormous scale [1]. In contrast with various methods to empirically estimate vaccine effectiveness VE , we know of no direct identification strategies for testing effectiveness (or similar quantities) in real-world settings. Complicating matters, our calculations suggest that any effective testing program will also shorten the generation interval and increase ascertainment, two quantities that impact the data and models underlying common estimators of the reproductive number R [52]. This suggests that an R -based empirical TE estimator would present challenges. Methodological development in this direction would be valuable.

Our modeling provides three potentially useful outputs beyond TE . First, we have attempted to quantify the twin costs of test consumption and isolation days, enabling the Pareto frontier between cost and benefit to be explored under a variety of assumptions. When weighted by dollar costs, these estimates may be useful for individuals and policymakers alike. Second, our calculations estimate ascertainment, which may be useful for surveillance and situational awareness. Third, the distribution of $t_{Dx} - TAT$, the post-exposure time at which the diagnosing test was taken, could be a valuable inclusion in “nowcasting” models, while the implied distribution of pathogen loads in diagnosing samples may be useful in estimating population-scale epidemiologic dynamics [53].

Our work is subject to a number of important limitations associated with the structure of our model. First, we assumed that symptoms may trigger testing, but do not trigger isolation in and of themselves. Relaxation of this assumption would require empirical estimates of self-isolation behavior or simply the additional assumption that a proportion of individuals directly isolate at symptom onset without testing [12]. Second, we modeled participation/refusal, compliance, and isolation behaviors as statistically independent between individuals, but health-related behaviors are known to be clustered [54–56], a type of heterogeneity not included in our TE calculations. In principle, estimates of TE for a set of behaviorally homogeneous groups could be computed and integrated into appropriately structured transmission models [51]. Finally, our model includes no treatment of specificity, an important factor for certain classes of diagnostic tests. The inclusion of imperfect specificity in our model would not affect TE estimates, but could substantially affect cost estimates, particularly if a low positive predictive value led to markedly more isolation days. For such scenarios, our model could be easily extended to include a second confirmatory test to derive a new distribution for t_{Dx} .

Our work is also subject to limitations associated with parameterization. For instance, we relied on estimates of pathogen load dynamics and symptom onset time, including variation thereof across a population. These are relatively well characterized for variants of SARS-CoV-2 in moderate to large population cohorts [16, 29,31,32,57], but are sparse for RSV [24,25] and influenza A [26–28] where they come typically from small numbers of healthy volunteers in human challenge studies and are typically presented through population means and confidence intervals, which, at best, indirectly inform between-host variation [58]. Even weakly characterized distributions are effectively unknown for many other pathogens, particularly prior to symptom onset. Joint estimates of viral kinetics and symptom prevalence and timing for many communicable diseases would be powerful for our modeling, and useful in many other applications as well, including studies of the value of early diagnosis as a path to timely treatment [18,19]. Extensions of this work to non-respiratory and non-human pathogens, particularly in agricultural settings, would be valuable. Another important limitation is the assumption that infectiousness can be parameterized as a function of the logarithm of viral load. While viral load and infectiousness are empirically linked in some studies [22,32,59], their precise relationship is more complicated. For instance, studies of SARS-COV-2 have shown fewer plaque-forming units per copy of viral RNA during an infection’s clearance phase than during its proliferation phase [45].

Finally, as with any public health intervention, there are important ethical considerations related to this work. This study focused on using resources (tests and isolation days) to provide a benefit (decreased transmission), yet not all individuals, communities, or settings may be equally well positioned to afford tests or isolation time. Similarly, our modeling focuses on population-scale transmission, but ignores heterogeneity in vulnerability among those to whom a disease may be transmitted. Finally, stigma around infection status could lead to low participation, particularly if that otherwise private status will be disclosed [60]. Application of this work should consider affordability, incentives, vulnerability, and privacy in local contexts.

Materials and Methods

Mathematical Model for Testing

We introduce testing effectiveness TE as the proportion by which a testing program decreases the risk of transmission, given infection, for an infectious disease [Eq. (1)] and define a mathematical model to prospectively estimate it. This model combines known or assumed properties of (i) a particular diagnostic test, (ii) a strategy for its administration, (iii) behavior/isolation after diagnosis, and (iv) the time-varying profiles of infectiousness and detectability over the course of an infection. Due to its integration of these elements, the model can also estimate a testing program's ascertainment (the proportion of infections detected), the impact of testing on the generation interval and selection coefficients, the distribution of diagnosis times, and the expected number of tests and isolation days required per diagnosis.

Infectiousness

In the absence of testing, the individual reproductive number ν_0 quantifies the expected number of secondary infections from that person [61], under typical behavior. It is given by the area under that individual's infectiousness curve $\beta(t)$ over time,

$$\nu_0 = \int_0^{\infty} \beta(t) dt . \quad (2)$$

The mean across all individual reproductive numbers is R by definition, and therefore

$$R_{\text{no testing}} = \mathbb{E}[\nu_0] = \int_0^{\infty} \mathbb{E}[\beta(t)] dt . \quad (3)$$

By prompting a post-diagnosis behavior change, participation in testing may isolate or attenuate part of that individual's infectiousness, decreasing its total from ν_0 to $\bar{\nu}_{\text{testing}}$. Provided that one's ν_0 and one's testing behaviors are statistically independent, then the mean across all individuals' $\bar{\nu}_{\text{testing}}$ is related to the effective reproductive number as

$$R_{\text{testing}} = p\mathbb{E}[\bar{\nu}_{\text{testing}}] + (1 - p)\mathbb{E}[\nu_0] , \quad (4)$$

where p represents the proportion of the population participating in testing. The participation rate incorporates both the proportion of the population that "opts in" to testing, as well as the fact that even among those opting in, not all will experience symptoms (for elective post-symptom testing) or be alerted to their having been exposed (for elective post-exposure testing). Our focus in the derivation that follows is to estimate $\bar{\nu}_{\text{testing}}$ for each person, after which we may average to get R_{testing} and thus TE .

Isolation after diagnosis

Suppose that at time t_{Dx} , an individual receives a diagnosis that causes them to attenuate their infectiousness via a change in behavior, such as isolation, masking, or increased ventilation. Here, we develop the mathematics corresponding to perfect isolation post-diagnosis, but provide equations for partial and/or time-varying impacts of behavior on transmission in Supplementary Materials. Post-diagnosis isolation leads to

$$\nu_{\text{testing}}(t_{Dx}) = \int_0^{t_{Dx}} \beta(t) dt + \int_{t_{\text{exit}}}^{\infty} \beta(t) dt , \quad (5)$$

which has the simple interpretation that one's infectiousness is simply that which occurred prior to diagnosis at t_{Dx} and that which occurred after exiting isolation at t_{exit} . While more complicated test-to-exit equations are developed in Supplementary Materials, here we consider only fixed isolation periods of duration ℓ , such that $t_{\text{exit}} = t_{Dx} + \ell$.

Time of diagnosis as a random variable. In practice, the time of diagnosis t_{Dx} depends on numerous factors including test availability or schedule or the timing of symptoms. We model t_{Dx} as a random variable with probability density function $f(t_{Dx})$. This leads to an effective infectiousness, calculated in expectation over the probable times of diagnosis, of

$$\bar{\nu}_{\text{testing}} = \int_0^{\infty} \nu_{\text{testing}}(t_{Dx}) f(t_{Dx}) dt_{Dx} . \quad (6)$$

Substituting in the definition of $\nu_{\text{testing}}(t_{Dx})$ from Eq. (S1), rearranging, and making use of the cumulative probability of a diagnosis $F(t)$,

$$\bar{\nu}_{\text{testing}} = \nu_0 - \int_0^{\infty} \beta(t) [F(t) - F(t - \ell)] dt . \quad (7)$$

We note that if one reinterprets $F(t)$ as the cumulative probability of symptom onset (as if symptoms were the diagnostic test itself), with an exhaustive isolation thereafter (large ℓ), then Eq. (7) recovers the core notion of symptom-based controllability of Fraser et al. [48]. However, unlike symptom onset, the time of diagnosis via testing t_{Dx} depends on within-host kinetics, test administration, and of course the test itself, as we calculate next.

Calculating t_{Dx} : testing, compliance, failure rates, detectability, and turnaround time

To calculate the distribution of diagnosis times $f(t_{Dx})$, we combine test administration—the probability that a test is administered at a particular time—and detection—the conditional probability that said test would return a positive diagnosis. This approach naturally separates a test administration strategy from the properties and performance of the particular diagnostic to be modeled.

Let $A(t)$ be the prescribed rate of test administration in tests per day, such that for sufficiently small δ ,

$$\Pr(\text{test administered between } t \text{ and } t + \delta) = \int_t^{t+\delta} A(t') dt' . \quad (8)$$

For instance, setting $A(t) = \frac{1}{7}$ would model a weekly screening regimen, while $A(t) = 2$ for $4 \leq t \leq 6$ would represent twice-daily testing starting 4 days post-exposure and ending on day 6.

Let $D(t)$ be an indicator function representing the analytical detectability of the infection at time t for a given diagnostic, such that $D(t) = 1$ when an infection is, in principle, detectable by that diagnostic, and $D(t) = 0$ otherwise. For example, to model qPCR, $D(t) = 1$ when concentrations of RNA or DNA from a biospecimen exceed the assay's limit of detection; below the limit of detection, $D(t) = 0$.

Combining administration with detectability, the cumulative number of scheduled tests with the potential to return a positive result by time t is

$$m(t) = \int_0^{t-\text{TAT}} A(t') D(t') dt' . \quad (9)$$

Note that the integral's upper limit is shifted by TAT, the test turnaround time, i.e., the amount of time between a test's administration and the return of actionable results. Although any particular person may have taken only an integer number of tests, $m(t)$ computes a real-valued expectation over all testing schedules or phases that match the specified rate $A(t)$.

The function $A(t)$ represents an *intended* test administration strategy (e.g., a policy or guideline), yet in many circumstances, imperfect compliance may result in missed tests. To account for compliance, we let c be the independent Bernoulli probability that each test is actually taken as intended.

Similarly, a test may fail for reasons unrelated to the analytical limit of detection or presence of a symptom. For example, poor biospecimen collection technique (e.g. poor nasal swab technique) could result in test failure irrespective of an assay's limit of detection [40]. To account for test failure of this type, we let ϕ be the independent Bernoulli probability that a test fails for non-analytical reasons.

Combining the number of possible positive tests taken $m(t)$ with compliance c and test failure ϕ , allows us to compute the cumulative probability that one has received a positive test by time t ,

$$F(t) = 1 - (1 - \bar{m}(t))[1 - c(1 - \phi)]^{m(t) - \bar{m}(t)} - \bar{m}(t)[1 - c(1 - \phi)]^{m(t) - \bar{m}(t) + 1} \quad (10)$$

where $\bar{m}(t) = m(t) \bmod 1$. We note that this is an improper CDF which need not reach 1 in the limit of large t , as not all individuals will necessarily receive a diagnosis. In the case where the product $A(t)D(t)$ is a constant \bar{A} between t_1 and t_2 , and 0 otherwise, the associated improper PDF is

$$f(t) = \bar{A}c(1 - \phi) (1 - c(1 - \phi))^{m(t) - \bar{m}(t)} \quad (11)$$

for $t_1 + \text{TAT} \leq t \leq t_2 + \text{TAT}$ and 0 otherwise.

In the specific case of elective testing at symptom onset, the functions above require slight modification to include the symptom onset time t_{Sx} . We modeled t_{Sx} as a random offset from the time of peak viral load, drawn from a specified uniform distribution (see Supplementary Table S1), a choice that reflects the way symptom onset is typically reported in the literature. For the cases considered in this manuscript, individuals wait x days after symptoms and test for y days at rate \bar{A} per day, leading to a test administration function,

$$A(t, t_{\text{Sx}}) = \bar{A} [u(t - t_{\text{Sx}} - x) - u(t - t_{\text{Sx}} - x - y)] , \quad (12)$$

where $u(t)$ is the unit step function defined as 0 prior to t and 1 thereafter. This equation means that Eq. (9) depends on t_{Sx} , and thus so does the cumulative probability of detection,

$$F(t, t_{\text{Sx}}) = 1 - (1 - \bar{m}(t, t_{\text{Sx}}))[1 - c(1 - \phi)]^{m(t, t_{\text{Sx}}) - \bar{m}(t, t_{\text{Sx}})} - \bar{m}(t, t_{\text{Sx}})[1 - c(1 - \phi)]^{m(t, t_{\text{Sx}}) - \bar{m}(t, t_{\text{Sx}}) + 1} . \quad (13)$$

The cumulative probability of detection can then be computed by integrating Eq. (13) against the t_{Sx} distribution.

Model Estimates

Testing effectiveness

Testing effectiveness TE can now be computed by substituting Eq. (7) ($\bar{\nu}_{\text{testing}}$) into Eq. (4) (R_{testing}) into Eq. (1), to get

$$TE = p \int_0^{\infty} \mathbb{E}[\beta(t) [F(t) - F(t - \ell)]] dt \Big/ \int_0^{\infty} \mathbb{E}[\beta(t)] dt, \quad (14)$$

where Eq. (10) can be used to compute the CDF $F(t)$ of diagnosis times t_{Dx} . If isolation is of sufficient duration to prevent all post-diagnosis transmission, TE simplifies to

$$TE = p \int_0^{\infty} \mathbb{E}[\beta(t)F(t)] dt \Big/ \int_0^{\infty} \mathbb{E}[\beta(t)] dt. \quad (15)$$

Note also that the integrands enclosed in expectations above have useful interpretations: they represent the expected infectiousness trajectories with (numerator) and without (denominator) participation in testing.

Ascertainment, and diagnosis and swab time distributions

For a single individual, the distribution of diagnosis times is given by its improper $f(t_{\text{Dx}})$ or CDF $F(t)$. The related improper distribution of “diagnosing swab” times is given by shifting the CDF by the turnaround time TAT.

The long-time limit of $F(t)$ is the probability that that individual will be diagnosed at all. Ascertainment, the proportion of infections diagnosed by a particular strategy at the population scale, can therefore be estimated by taking the expectation of the long-time limits over individuals, and scaling by the participation rate,

$$\alpha = p \lim_{t \rightarrow \infty} \mathbb{E}[F(t)]. \quad (16)$$

Here, the expectation is taken over individual heterogeneity in within-host dynamics across the population (just as in Eqs. (3) and (4)).

Mean generation interval and selection coefficient

The mean generation interval, defined as the typical time between infection and subsequent transmission, can be computed from the centers of mass of the expected infectiousness curves that appear in the numerator and denominator of Eq. (S3). Such estimates may be important for post-hoc estimation of TE from empirical data, given that methods of estimating R_t from empirical case counts often rely on the mean generation interval.

If a single test is capable of diagnosing two strains of the same pathogen, then there is the potential for testing to alter the selection coefficient. Here, TE calculations can estimate this impact, such that the selection coefficient is predicted to shift from $s = \frac{R_A}{R_B}$ to $s_{\text{testing}} = s \frac{(1-TE_A)}{(1-TE_B)}$.

Test Consumption

How many tests are consumed during the course of a testing regimen? We break this calculation into two cases, depending on whether the individual receives a diagnosis or not.

First, suppose an individual never tests positive. This implies that any tests that were meant to be taken when the infection was detectable, i.e. when $D(t) = 1$, were either (i) not taken, due to a failure of compliance (probability $1 - c$), or (ii) taken yet failed to provide the correct positive diagnosis (probability $c\phi$). Because only the latter case consumes a test, this means that a key quantity is $c\phi/(1 - c + c\phi)$, the relative probability that a planned test consumed a test, given the absence of diagnosis. On the other hand, any tests meant to be taken when the infection was undetectable, i.e. when $D(t) = 0$, were taken with probability c . Summing these two provides an estimate of average test consumption for those who are not diagnosed.

$$\bar{q}_{\text{no-Dx}} = \frac{c\phi}{1 - c + c\phi} \int_0^\infty A(t)D(t) dt + c \int_0^\infty A(t) [1 - D(t)] dt. \quad (17)$$

The reason that we call this an estimate and not an exact calculation is that testing and diagnosis are causally linked, and therefore conditioning on a no-diagnosis outcome means that the prescribed test administration may no longer be $A(t)$ exactly.

In contrast, if an individual receives a diagnosis at t_{Dx} , we assume that no additional tests were consumed thereafter, and that at least one test was consumed—if not, no diagnosis could have been produced. For a fixed time of diagnosis,

$$q_{\text{Dx}}(t_{\text{Dx}}) = 1 + c \left[\int_0^{t_{\text{Dx}} - \text{TAT}} A(t) dt + \int_{t_{\text{Dx}} - \text{TAT}}^{t_{\text{Dx}}} A(t) dt \right]. \quad (18)$$

Above, the first integral accounts for non-diagnostic test consumption up until the diagnosing test, while the second integral accounts for additional tests consumed while waiting for the diagnosing test. The separate floor functions are a necessary consequence of conditioning on the separate counting of the diagnosing test. Taking an expectation over t_{Dx} yields

$$\bar{q}_{\text{Dx}} = 1 + \frac{pc}{\alpha} \left[\int_0^\infty \left[\int_0^{t_{\text{Dx}} - \text{TAT}} A(t) dt \right] f(t_{\text{Dx}}) dt_{\text{Dx}} + \int_0^\infty \left[\int_{t_{\text{Dx}} - \text{TAT}}^{t_{\text{Dx}}} A(t) dt \right] f(t_{\text{Dx}}) dt_{\text{Dx}} \right]. \quad (19)$$

Combining our calculations for $\bar{q}_{\text{no-Dx}}$ and \bar{q}_{Dx} , weighting the latter by ascertainment and the former by its complement, we get a general expression for the expected test consumption among infected individuals,

$$\bar{q}_{\text{infected}} = (1 - \alpha) \bar{q}_{\text{no-Dx}} + \alpha \bar{q}_{\text{Dx}}. \quad (20)$$

Of course, the whole point of testing is that one does not know *a priori* who is infected and who is not. Consequently, we can estimate consumption by those who are not infected as

$$\bar{q}_{\text{not infected}} = c \int_0^\infty A(t) dt. \quad (21)$$

Finally, combining Eqs. (20) and (21), we get

$$Q = p \left[(\theta \text{se}_{\text{ref.}}) \bar{q}_{\text{infected}} + (1 - \theta)(1 - \text{sp}_{\text{ref.}}) \bar{q}_{\text{not infected}} \right], \quad (22)$$

where p is the population participation rate, θ is the prevalence of the pathogen, and $\text{se}_{\text{ref.}}$ and $\text{sp}_{\text{ref.}}$ are the sensitivity and specificity of the scheme used to refer people to testing, respectively. Such referral schemes include contact tracing, the appearance of symptoms, membership in a group with known high risk of infection, or even universal testing (in which case the referral “program” would have $\text{se} = 1$ and $\text{sp} = 0$).

Days spent in isolation

For fixed-duration perfect isolation of length ℓ , the average number of isolation days per infected person is given by the product of ℓ and ascertainment $d = \ell \alpha$. A similar calculation for test-to-exit policies is found in Supplementary Equation (S10).

Parameterization of the Model

Viral kinetics, symptoms onset, and infectiousness

We parameterized the time-varying profiles of viral load and infectiousness using a simplified model which captures four features common to RSV [24], influenza A [26], and multiple variants of SARS-CoV-2 [16]: (i) a post-exposure period where virus is undetectable by any known test, (ii) a proliferation period of exponential growth, (iii) a peak viral load (VL), followed by (iv) a clearance period of exponential decline. We capture these features using a piecewise linear “tent” function specified by three points: (t_0, LLOQ) , the first time at which VL exceeds the lower limit of quantification (LLOQ); $(t_{\text{peak}}, V_{\text{peak}})$, peak VL timing and concentration; and (t_f, LLOQ) , the last detectable time [12, 16], where t represents the time since exposure in days. Because within-host kinetics vary from one infection to another, each trajectory is parameterized using independent draws from random variables for each control point.

While summarized in Supplementary Table S1, we briefly review the studies and sources of evidence used to parameterize our simple viral load models. Influenza A latent period parameters were drawn from a review of challenge studies by Carrat et al. supporting a 0.5–2d delay between inoculation and first detectable instance using a gold standard test [26], noting that this range is slightly wider than in other studies [27]. Data from a household study from Ip et al. characterized peak VL between 1–3d after symptom onset, and noted that symptom onset and first detectability were indistinguishable. Their data also showed peak VL between 6–8.5 \log_{10} cp RNA/mL, followed by 2–3d clearance times [28]. We note that these clearance times were shorter than those observed in challenge studies [26, 27]. Symptom onset time was specified as taking place between 2d and 0d prior to peak VL from observations of naturally acquired infection [34].

RSV viral kinetics were characterized using vaccine efficacy challenge studies, which reported only geometric means of viral load, measured in days since challenge inoculation [24, 25]. Placebo group data from both studies support a 2–4d latent period and 3–6d between peak VL and clearance [24, 25]. Schmoele-Thoma et al. present individual data points for longitudinal sampling of infected participants supporting a proliferation phase of 2–4d and peak VL between 4.5–8 \log_{10} cp RNA/mL [24]. Sadoff et al. indicate slightly later and lower peaks, but we weight these less heavily in model parameterization because only mean and confidence intervals are presented, but not individual data points [25]. Symptom onset time was specified as taking place between 1d prior to and 1d after peak VL from an additional human challenge study [62].

We briefly note that our characterization of influenza A and RSV viral kinetics relies primarily on studies meant to capture vaccine [24, 25] and drug [27] efficacy, or to report symptom dynamics [28]. In all four studies, viral kinetics data are reported as a secondary finding, and typically as a geometric mean since time of onset—including, in two instances, all the individuals for whom inoculation failed [24, 25]. Due to the lack of viral load data linked at the level of individuals to inform distributional choices of kinetics parameters across a population, we assumed uniform distributions over supported parameter ranges for both viruses.

In contrast, our estimates of SARS-CoV-2 viral kinetics parameters were drawn from studies performed specifically to characterize within-host viral dynamics. Kissler et al. and Hay et al. provide mean and 95% credible interval estimates for peak VL and the durations of the proliferation and clearance phases for

founder-strain/naive and omicron-strain/experienced SARS-CoV-2, respectively [16, 30]. Parameter distributions were assumed to be Lognormal with parameters μ and σ , whose values were adapted from published means, 95% credible intervals, and sample sizes. Specifically, we selected values such that an equal number of draws from $\text{Lognormal}(\mu, \sigma)$ would lead to a frequentist confidence interval matching the published mean and credible interval to the closest approximation. See Table S1 for these parameter values. Given the possibility of the occasional non-biologically large draw from the Lognormal distributions, we rejected proliferation phases shorter than 0.5d and longer than 10d, and rejected clearance phases shorter than 0.5d and longer than 25d for both SARS-CoV-2 models. A challenge study provides support for a 2.5-3.5d latent period after inoculation [29]. Symptom onset time was specified as taking place between 0-3d after peak VL for founder-strain/naive infections [30, 44, 45], and between 1-5d before peak VL for omicron-variant/experienced infections [29, 63, 64].

Given a stochastic realization of viral kinetics from the model above, we calculated infectiousness $\beta(t)$ as proportional to the logarithm of viral load in excess of some minimum threshold, specified by the typical viral load (concentration of RNA cpRNA/ml) at which plaque forming units are consistently found (> 1 PFU/ml). While this type of log-viral-load infectiousness assumption is common for studies of influenza A [26, 65], SARS-CoV-2 [47], and RSV [66], alternative relationships between viral load (or other quantities) and infectiousness are possible [12, 67].

Analytical sensitivity and failure rate of diagnostic tests

Analytical sensitivities (limits of detection; LODs) were drawn from the literature for RT-qPCR and RDT tests for influenza A, RSV, founder-strain SARS-CoV-2, and SARS-CoV-2 omicron variants. Due to the variability in LODs between assays of the same type for the same pathogen, we chose a single value (Table S1) to represent each pathogen and test type. Above a test's estimated LOD, false negative rates ϕ were available only for SARS-CoV-2 [40] at approximately 5%, a rate we assumed for RSV and influenza A, collectively modeling factors such as sample contamination, poor biospecimen collection, or manufacturing error. In general, parameters were more widely available and better characterized for SARS-CoV-2 tests than for RSV or influenza A. See Table S1 for LODs, failure rates, and relevant sources.

Acknowledgements

The authors wish to thank the BioFrontiers Institute IT HPC group, Yonatan Grad, Sarah Cobey, and Stephen Kissler. C.E.M. was supported in part by the Interdisciplinary Quantitative Biology (IQBio) program at the University of Colorado Boulder and by the SeroNet program of the National Cancer Institute (1U01CA261277-01). D.B.L. was supported in part by an NSF Alan T. Waterman Award (SMA-2226343).

Author Contributions

C.E.M. and D.B.L. conceived of and designed the study, derived the model, and wrote the manuscript. C.E.M. conducted extensive literature reviews to parameterize models, and conducted numerical simulations.

Code Availability

All code needed to evaluate the conclusions in the paper are present in the paper and/or the Supplementary Materials, and open-source code (Python 3.7.4) is available at <https://github.com/CaseyMiddleton/TestingFramework>.

Data Availability

No datasets were generated or analysed during the current study.

Competing Interests

D.B.L. is a member of the scientific advisory board of Darwin BioSciences and discloses past consulting for Flambeau RapidX.

References

- [1] Brian E McGarry, Ashvin D Gandhi, and Michael L Barnett. COVID-19 surveillance testing and resident outcomes in nursing homes. *New England Journal of Medicine*, 388(12):1101–1110, 2023.
- [2] Diana Rose E Ranoa, Robin L Holland, Fadi G Alnaji, Kelsie J Green, Leyi Wang, Richard L Fredrickson, Tong Wang, George N Wong, Johnny Uelmen, Sergei Maslov, et al. Mitigation of SARS-CoV-2 transmission at a large public university. *Nature Communications*, 13(1):3207, 2022.
- [3] Martin Pavelka, Kevin Van-Zandvoort, Sam Abbott, Katharine Sherratt, Marek Majdan, CM-MID COVID-19 working group, Inštitút Zdravotných Analýz, Pavol Jarčuška, Marek Krajčák, Stefan Flasche, and Sebastian Funk. The impact of population-wide rapid antigen testing on SARS-CoV-2 prevalence in slovakia. *Science*, 372(6542):635–641, 2021.
- [4] David I Bernstein, Asuncion Mejias, Barbara Rath, Christopher W Woods, and Jamie Phillips Deeter. Summarizing study characteristics and diagnostic performance of commercially available tests for respiratory syncytial virus: A scoping literature review in the COVID-19 era. *The Journal of Applied Laboratory Medicine*, 8(2):353–371, 2023.
- [5] Joanna Merckx, Rehab Wali, Ian Schiller, Chelsea Caya, Genevieve C Gore, Caroline Chartrand, Nandini Dendukuri, and Jesse Papenburg. Diagnostic accuracy of novel and traditional rapid tests for influenza infection compared with reverse transcriptase polymerase chain reaction: a systematic review and meta-analysis. *Annals of Internal Medicine*, 167(6):394–409, 2017.
- [6] Dishit P Ghumra, Nishit Shetty, Kevin R McBrearty, Joseph V Puthussery, Benjamin J Sumlin, Woodrow D Gardiner, Brookelyn M Doherty, Jordan P Magrecki, David L Brody, Thomas J Esparza, et al. Rapid direct detection of SARS-CoV-2 aerosols in exhaled breath at the point of care. *ACS Sensors*, 2023.
- [7] Hsing-Yi Chung, Ming-Jr Jian, Chih-Kai Chang, Jung-Chung Lin, Kuo-Ming Yeh, Chien-Wen Chen, Sheng-Kang Chiu, Yi-Hui Wang, Shu-Jung Liao, Shih-Yi Li, et al. Novel dual multiplex real-time rt-pcr assays for the rapid detection of SARS-CoV-2, influenza A/B, and respiratory syncytial virus using the bd max open system. *Emerging Microbes & Infections*, 10(1):161–166, 2021.
- [8] Salim Ferrani, Thierry Prazuck, Stéphane Béchet, Fabien Lesne, Robert Cohen, and Corinne Levy. Diagnostic accuracy of a rapid antigen triple test (SARS-CoV-2, respiratory syncytial virus, and influenza) using anterior nasal swabs versus multiplex rt-pcr in children in an emergency department. *Infectious Diseases Now*, page 104769, 2023.
- [9] Jason S Haukoos, Emily Hopkins, Amy A Conroy, Morgan Silverman, Richard L Byyny, Sheri Eisert, Mark W Thrun, Michael L Wilson, Angela B Hutchinson, Jessica Forsyth, et al. Routine opt-out rapid

- hiv screening and detection of hiv infection in emergency department patients. *Jama*, 304(3):284–292, 2010.
- [10] Sindew M Feleke, Emily N Reichert, Hussein Mohammed, Bokretsion G Brhane, Kalkidan Mekete, Hassen Mamo, Beyene Petros, Hiwot Solomon, Ebba Abate, Chris Hennelly, et al. Plasmodium falciparum is evolving to escape malaria rapid diagnostic tests in ethiopia. *Nature Microbiology*, 6(10):1289–1299, 2021.
- [11] A David Paltiel, Amy Zheng, and Rochelle P Walensky. Assessment of SARS-CoV-2 screening strategies to permit the safe reopening of college campuses in the united states. *JAMA Network Open*, 3(7):e2016818–e2016818, 2020.
- [12] Daniel B. Larremore, Bryan Wilder, Evan Lester, Soraya Shehata, James M. Burke, James A. Hay, Milind Tambe, Michael J. Mina, and Roy Parker. Test sensitivity is secondary to frequency and turnaround time for COVID-19 screening. *Science Advances*, 7(1), January 1 2021.
- [13] Ted Bergstrom, Carl T Bergstrom, and Haoran Li. Frequency and accuracy of proactive testing for COVID-19. *MedRxiv*, pages 2020–09, 2020.
- [14] Nicholas C Grassly, Margarita Pons-Salort, Edward PK Parker, Peter J White, Neil M Ferguson, Kylie Ainslie, Marc Baguelin, Samir Bhatt, Adhiratha Boonyasiri, Nick Brazeau, et al. Comparison of molecular testing strategies for COVID-19 control: a mathematical modelling study. *The Lancet Infectious Diseases*, 20(12):1381–1389, 2020.
- [15] Adam J Kucharski, Petra Klepac, Andrew JK Conlan, Stephen M Kissler, Maria L Tang, Hannah Fry, Julia R Gog, W John Edmunds, Jon C Emery, Graham Medley, et al. Effectiveness of isolation, testing, contact tracing, and physical distancing on reducing transmission of SARS-CoV-2 in different settings: a mathematical modelling study. *The Lancet Infectious Diseases*, 20(10):1151–1160, 2020.
- [16] Stephen M. Kissler, Joseph R. Fauver, Christina Mack, Scott W. Olesen, Caroline Tai, Kristin Y. Shiue, Chaney C. Kalinich, Sarah Jednak, Isabel M. Ott, Chantal B. F. Vogels, Jay Wohlgemuth, James Weisberger, John DiFiori, Deverick J. Anderson, Jimmie Mancell, David D. Ho, Nathan D. Grubaugh, and Yonatan H. Grad. Viral dynamics of acute SARS-CoV-2 infection and applications to diagnostic and public health strategies. *PLOS Biology*, 19(7):1–17, 07 2021.
- [17] Inga Holmdahl, Rebecca Kahn, James A Hay, Caroline O Buckee, and Michael J Mina. Estimation of transmission of COVID-19 in simulated nursing homes with frequent testing and immunity-based staffing. *JAMA Network Open*, 4(5):e2110071–e2110071, 2021.
- [18] Tigist F Menkir and Christl A Donnelly. The impact of repeated rapid test strategies on the effectiveness of at-home antiviral treatments for SARS-CoV-2. *Nature Communications*, 13(1):5283, 2022.
- [19] Shengyuan Zhang, Akosua A Agyeman, Christoforos Hadjichrysanthou, and Joseph F Standing. SARS-CoV-2 viral dynamic modelling to inform model selection and timing and efficacy of antiviral therapy. *CPT: Pharmacometrics & Systems Pharmacology*, 2023.
- [20] James M Hyman, Jia Li, and E Ann Stanley. Modeling the impact of random screening and contact tracing in reducing the spread of hiv. *Mathematical biosciences*, 181(1):17–54, 2003.
- [21] Yazdan Yazdanpanah, Caroline E Sloan, Cécile Charlois-Ou, Stéphane Le Vu, Caroline Semaille, Dominique Costagliola, Josiane Pilonel, Anne-Isabelle Poullié, Olivier Scemama, Sylvie Deuffic-

- Burban, et al. Routine hiv screening in france: clinical impact and cost-effectiveness. *PloS one*, 5(10):e13132, 2010.
- [22] Kristen K Bjorkman, Tassa K Saldi, Erika Lasda, Leisha Conners Bauer, Jennifer Kovarik, Patrick K Gonzales, Morgan R Fink, Kimngan L Tat, Cole R Hager, Jack C Davis, et al. Higher viral load drives infrequent severe acute respiratory syndrome coronavirus 2 transmission between asymptomatic residence hall roommates. *The Journal of Infectious Diseases*, 224(8):1316–1324, 2021.
- [23] Louise E Smith, R Amlôt, Helen Lambert, Isabel Oliver, Charlotte Robin, Lucy Yardley, and G James Rubin. Factors associated with adherence to self-isolation and lockdown measures in the uk: a cross-sectional survey. *Public Health*, 187:41–52, 2020.
- [24] Beate Schmoele-Thoma, Agnieszka M. Zareba, Qin Jiang, Mohan S. Maddur, Rana Danaf, Alex Mann, Kingsley Eze, Juin Fok-Seang, Golam Kabir, Andrew Catchpole, Daniel A. Scott, Alejandra C. Gurtman, Kathrin U. Jansen, William C. Gruber, Philip R. Dormitzer, and Kena A. Swanson. Vaccine efficacy in adults in a respiratory syncytial virus challenge study. *New England Journal of Medicine*, 386(25):2377–2386, Jun 2022.
- [25] Jerald Sadoff, Els De Paepe, John DeVincenzo, Efi Gymnopoulou, Joris Menten, Bryan Murray, Arangassery Rosemary Bastian, An Vandebosch, Wouter Haazen, Nicolas Noulin, Christy Comeaux, Esther Heijnen, Kingsley Eze, Anthony Gilbert, Rob Lambkin-Williams, Hanneke Schuitemaker, and Benoit Callendret. Prevention of respiratory syncytial virus infection in healthy adults by a single immunization of Ad26.RSV.preF in a human challenge study. *The Journal of Infectious Diseases*, 226(3):396–406, Jan 2021.
- [26] Fabrice Carrat, Elisabeta Vergu, Neil M. Ferguson, Magali Lemaitre, Simon Cauchemez, Steve Leach, and Alain-Jacques Valleron. Time Lines of Infection and Disease in Human Influenza: A Review of Volunteer Challenge Studies. *American Journal of Epidemiology*, 167(7):775–785, 01 2008.
- [27] Susan E. Sloan, Kristy J. Szretter, Bharathi Sundaresh, Kristin M. Narayan, Patrick F. Smith, David Skurnik, Sylvain Bedard, José M. Trevejo, David Oldach, and Zachary Shriver. Clinical and virological responses to a broad-spectrum human monoclonal antibody in an influenza virus challenge study. *Antiviral Research*, 184:104763, Dec 2020.
- [28] Dennis K. M. Ip, Lincoln L. H. Lau, Kwok-Hung Chan, Vicky J. Fang, Gabriel M. Leung, Malik J. S. Peiris, and Benjamin J. Cowling. The dynamic relationship between clinical symptomatology and viral shedding in naturally acquired seasonal and pandemic influenza virus infections. *Clinical Infectious Diseases*, 62(4):431–437, Feb 2016.
- [29] Ben Killingley, Alex J Mann, Mariya Kalinova, Alison Boyers, Niluka Goonawardane, Jie Zhou, Kate Lindsell, Samanjit S Hare, Jonathan Brown, Rebecca Frise, et al. Safety, tolerability and viral kinetics during SARS-CoV-2 human challenge in young adults. *Nature Medicine*, 28(5):1031–1041, 2022.
- [30] James A Hay, Stephen M Kissler, Joseph R Fauver, Christina Mack, et al. Quantifying the impact of immune history and variant on SARS-CoV-2 viral kinetics and infection rebound: A retrospective cohort study. *eLife*, 11:e81849, Nov 2022.
- [31] Ruian Ke, Carolin Zitzmann, David D. Ho, Ruy M. Ribeiro, and Alan S. Perelson. In vivo kinetics of SARS-CoV-2 infection and its relationship with a person’s infectiousness. *Proceedings of the National Academy of Sciences*, 118(49):e2111477118, Dec 2021.

- [32] Ruian Ke, Pamela P Martinez, Rebecca L Smith, Laura L Gibson, Agha Mirza, Madison Conte, Nicholas Gallagher, Chun Huai Luo, Junko Jarrett, Ruifeng Zhou, et al. Daily longitudinal sampling of SARS-CoV-2 infection reveals substantial heterogeneity in infectiousness. *Nature Microbiology*, 7(5):640–652, 2022.
- [33] Joseph Sriyal Malik Peiris, Chung-Ming Chu, Vincent Chi-Chung Cheng, KS Chan, IFN Hung, Leo LM Poon, Kin-Ip Law, BSF Tang, TYW Hon, CS Chan, et al. Clinical progression and viral load in a community outbreak of coronavirus-associated SARS pneumonia: a prospective study. *The Lancet*, 361(9371):1767–1772, 2003.
- [34] Lincoln L. H. Lau, Benjamin J. Cowling, Vicky J. Fang, Kwok-Hung Chan, Eric H. Y. Lau, Marc Lipsitch, Calvin K. Y. Cheng, Peter M. Houch, Timothy M. Uyeki, J. S. Malik Peiris, and Gabriel M. Leung. Viral shedding and clinical illness in naturally acquired influenza virus infections. *The Journal of Infectious Diseases*, 201(10):1509–1516, 05 2010.
- [35] Patrick K. Munywoki, Dorothy C. Koech, Charles N. Agoti, Ann Bett, Patricia A. Cane, Graham F. Medley, and D. James Nokes. Frequent asymptomatic respiratory syncytial virus infections during an epidemic in a rural Kenyan household cohort. *The Journal of Infectious Diseases*, 212(11):1711–1718, Dec 2015.
- [36] Cost-Effectiveness of Preventing AIDS Complications (CEPAC) model.
- [37] Statement on the fifteenth meeting of the IHR (2005) emergency committee on the COVID-19 pandemic. [https://www.who.int/news/item/05-05-2023-statement-on-the-fifteenth-meeting-of-the-international-health-regulations-\(2005\)-emergency-committee-regarding-the-coronavirus-disease-\(COVID-19\)-pandemic](https://www.who.int/news/item/05-05-2023-statement-on-the-fifteenth-meeting-of-the-international-health-regulations-(2005)-emergency-committee-regarding-the-coronavirus-disease-(COVID-19)-pandemic), May 5, 2023.
- [38] Preliminary estimated influenza illnesses, medical visits, hospitalizations, and deaths in the united states – 2021-2022 influenza season. <https://www.cdc.gov/flu/about/burden/2021-2022.htm>, October 4, 2022.
- [39] You Li, Xin Wang, Dianna M Blau, Mauricio T Caballero, Daniel R Feikin, Christopher J Gill, Shabir A Madhi, Saad B Omer, Eric AF Simões, Harry Campbell, et al. Global, regional, and national disease burden estimates of acute lower respiratory infections due to respiratory syncytial virus in children younger than 5 years in 2019: a systematic analysis. *The Lancet*, 399(10340):2047–2064, 2022.
- [40] Jean-Louis Bayart, Jonathan Degosserie, Julien Favresse, Constant Gillot, Marie Didembourg, Happy Phanio Djokoto, Valérie Verbelen, Gatién Roussel, Céline Maschietto, François Mullier, Jean-Michel Dogné, and Jonathan Douxfils. Analytical sensitivity of six SARS-CoV-2 rapid antigen tests for omicron versus delta variant. *Viruses*, 14(44):654, Apr 2022.
- [41] Meriem Bekliz, Kenneth Adea, Olha Puhach, Francisco Perez-Rodriguez, Stéfane Marques Melancia, Stephanie Baggio, Anna-Rita Corvaglia, Frederique Jacqueroiz, Catia Alvarez, Manel Essaidi-Laziosi, Camille Escadafal, Laurent Kaiser, and Isabella Eckerle. Analytical sensitivity of eight different SARS-CoV-2 antigen-detecting rapid tests for omicron-ba.1 variant. *Microbiology Spectrum*, 10(4):e00853–22, Aug 2022.

- [42] Cara E. Brook, Graham R. Northrup, Alexander J. Ehrenberg, Jennifer A. Doudna, and Mike Boots. Optimizing COVID-19 control with asymptomatic surveillance testing in a university environment. *Epidemics*, 37:100527, Dec 2021.
- [43] Michael J Mina, Roy Parker, and Daniel B Larremore. Rethinking COVID-19 test sensitivity—a strategy for containment. *New England Journal of Medicine*, 383(22):e120, 2020.
- [44] Ingrid Torjesen. COVID-19: Peak of viral shedding is later with omicron variant, japanese data suggest. *BMJ*, 376:89, Jan 2022.
- [45] Seran Hakki, Jie Zhou, Jakob Jonnerby, Anika Singanayagam, Jack L Barnett, Kieran J Madon, Aleksandra Koycheva, Christine Kelly, Hamish Houston, Sean Nevin, Joe Fenn, Rhia Kundu, Michael A Crone, Timesh D Pillay, Shazaad Ahmad, Nieves Derqui-Fernandez, Emily Conibear, Paul S Freemont, Graham P Taylor, Neil Ferguson, Maria Zambon, Wendy S Barclay, Jake Dunning, Ajit Lalvani, Anjna Badhan, Robert Varro, Constanta Luca, Valerie Quinn, Jessica Cutajar, Niamh Nichols, Jessica Russell, Holly Grey, Anjeli Ketkar, Giulia Miserochi, Chitra Tejpal, Harriet Catchpole, Koji Nixon, Berenice Di Biase, Tamara Hopewell, Janakan Sam Narean, Jada Samuel, Kristel Timcang, Eimear McDermott, Samuel Bremang, Sarah Hammett, Samuel Evetts, and Alexandra Kondratiuk. Onset and window of SARS-CoV-2 infectiousness and temporal correlation with symptom onset: a prospective, longitudinal, community cohort study. *The Lancet Respiratory Medicine*, 10(11):1061–1073, Nov 2022.
- [46] Isolation and precautions for people with COVID-19. <https://www.cdc.gov/coronavirus/2019-ncov/your-health/isolation.html>, May 11, 2023.
- [47] Daniel Larremore, Derek Toomre, and Roy Parker. Modeling the effectiveness of olfactory testing to limit SARS-CoV-2 transmission. *Nature Communications*, 12(1), June 16 2021.
- [48] Christophe Fraser, Steven Riley, Roy M Anderson, and Neil M Ferguson. Factors that make an infectious disease outbreak controllable. *Proceedings of the National Academy of Sciences*, 101(16):6146–6151, 2004.
- [49] Joel Hellewell, Sam Abbott, Amy Gimma, Nikos I Bosse, Christopher I Jarvis, Timothy W Russell, James D Munday, Adam J Kucharski, W John Edmunds, Fiona Sun, et al. Feasibility of controlling COVID-19 outbreaks by isolation of cases and contacts. *The Lancet Global Health*, 8(4):e488–e496, 2020.
- [50] Kate M. Bubar, Kyle Reinholt, Stephen M. Kissler, Marc Lipsitch, Sarah Cobey, Yonatan H. Grad, and Daniel B. Larremore. Model-informed COVID-19 vaccine prioritization strategies by age and serostatus. *Science*, 371(6532):916–921, Feb 2021.
- [51] Kate M Bubar, Casey E Middleton, Kristen K Bjorkman, Roy Parker, and Daniel B Larremore. SARS-CoV-2 transmission and impacts of unvaccinated-only screening in populations of mixed vaccination status. *Nature Communications*, 13(2777), 2022.
- [52] Jacco Wallinga and Peter Teunis. Different epidemic curves for severe acute respiratory syndrome reveal similar impacts of control measures. *American Journal of Epidemiology*, 160(6):509–516, 2004.
- [53] James A Hay, Lee Kennedy-Shaffer, Sanjat Kanjilal, Niall J Lennon, Stacey B Gabriel, Marc Lipsitch, and Michael J Mina. Estimating epidemiologic dynamics from cross-sectional viral load distributions. *Science*, 373(6552):eabh0635, 2021.

- [54] Tracy A Lieu, G Thomas Ray, Nicola P Klein, Cindy Chung, and Martin Kulldorff. Geographic clusters in underimmunization and vaccine refusal. *Pediatrics*, 135(2):280–289, 2015.
- [55] Stephen M Kissler, Nishant Kishore, Malavika Prabhu, Dena Goffman, Yaakov Beilin, Ruth Landau, Cynthia Gyamfi-Bannerman, Brian T Bateman, Jon Snyder, Armin S Razavi, et al. Reductions in commuting mobility correlate with geographic differences in SARS-CoV-2 prevalence in new york city. *Nature Communications*, 11(1):4674, 2020.
- [56] David Holtz, Michael Zhao, Seth G Benzell, Cathy Y Cao, Mohammad Amin Rahimian, Jeremy Yang, Jennifer Allen, Avinash Collis, Alex Moehring, Tara Sowrirajan, et al. Interdependence and the cost of uncoordinated responses to COVID-19. *Proceedings of the National Academy of Sciences*, 117(33):19837–19843, 2020.
- [57] Timothy W Russell, Hermaleigh Townsley, Sam Abbott, Joel Hellewell, Edward J Carr, Lloyd Chapman, Rachael Pung, Billy J Quilty, David Hodgson, Ashley Fowler, et al. Within-host SARS-CoV-2 viral kinetics informed by complex life course exposures reveals different intrinsic properties of omicron and delta variants. *medRxiv*, pages 2023–05, 2023.
- [58] Sam Zhang, Patrick R. Heck, Michelle N. Meyer, Christopher F. Chabris, Daniel G. Goldstein, and Jake M. Hofman. An illusion of predictability in scientific results: Even experts confuse inferential uncertainty and outcome variability. *Proceedings of the National Academy of Sciences*, 120(33):e2302491120, 2023.
- [59] Terry C. Jones, Guido Biele, Barbara Mühlemann, Talitha Veith, Julia Schneider, Jörn Beheim-Schwarzbach, Tobias Bleicker, Julia Tesch, Marie Luisa Schmidt, Leif Erik Sander, Florian Kurth, Peter Menzel, Rolf Schwarzer, Marta Zuchowski, Jörg Hofmann, Andi Krumbholz, Angela Stein, Anke Edelmann, Victor Max Corman, and Christian Drosten. Estimating infectiousness throughout SARS-CoV-2 infection course. *Science*, 373(6551), Jul 2021.
- [60] Suzanne E Landis, Victor J Schoenbach, David J Weber, Manjoo Mittal, Baldev Krishan, Karen Lewis, and Gary G Koch. Results of a randomized trial of partner notification in cases of hiv infection in north carolina. *New england Journal of medicine*, 326(2):101–106, 1992.
- [61] James O Lloyd-Smith, Sebastian J Schreiber, P Ekkehard Kopp, and Wayne M Getz. Superspreading and the effect of individual variation on disease emergence. *Nature*, 438(7066):355–359, 2005.
- [62] F.Eun-Hyung Lee, Edward E. Walsh, Ann R. Falsey, Robert F. Betts, and John J. Treanor. Experimental infection of humans with A2 respiratory syncytial virus. *Antiviral Research*, 63(3):191–196, 2004.
- [63] Nadège Néant, Guillaume Lingas, Quentin Le Hingrat, Jade Ghosn, Ilka Engelmann, Quentin Lepiller, Alexandre Gaymard, Virginie Ferré, Cédric Hartard, Jean-Christophe Plantier, Vincent Thibault, Julien Marlet, Brigitte Montes, Kevin Bouiller, François-Xavier Lescure, Jean-François Timsit, Emmanuel Faure, Julien Poissy, Christian Chidiac, François Raffi, Antoine Kimmoun, Manuel Etienne, Jean-Christophe Richard, Pierre Tattevin, Denis Garot, Vincent Le Moing, Delphine Bachelet, Coralie Tardivon, Xavier Duval, Yazdan Yazdanpanah, France Mentré, Cédric Laouénan, Benoit Visseaux, Jérémie Guedj, French COVID Cohort Investigators, and French Cohort Study groups. Modeling SARS-CoV-2 viral kinetics and association with mortality in hospitalized patients from the French COVID cohort. *Proceedings of the National Academy of Sciences of the United States of America*, 118(8):e2017962118, Feb 2021.

- [64] Lauren M. Kucirka, Stephen A. Lauer, Oliver Laeyendecker, Denali Boon, and Justin Lessler. Variation in false-negative rate of reverse transcriptase polymerase chain reaction–based SARS-CoV-2 tests by time since exposure. *Annals of Internal Medicine*, 173(4):262–267, 2020. PMID: 32422057.
- [65] Hana M. Dobrovolny, Micaela B. Reddy, Mohamed A. Kamal, Craig R. Rayner, and Catherine A. A. Beauchemin. Assessing mathematical models of influenza infections using features of the immune response. *PLOS ONE*, 8(2):1–20, 02 2013.
- [66] M Wathuo, GF Medley, DJ Nokes, and PK Munywoki. Quantification and determinants of the amount of respiratory syncytial virus (RSV) shed using real time PCR data from a longitudinal household study [version 2; peer review: 3 approved, 1 approved with reservations]. *Wellcome Open Res*, 1(27), 2017.
- [67] Ruian Ke, Pamela P. Martinez, Rebecca L. Smith, Laura L. Gibson, Chad J. Achenbach, Sally McFall, Chao Qi, Joshua Jacob, Etienne Dembele, Camille Bundy, Lacy M. Simons, Egon A. Ozer, Judd F. Hultquist, Ramon Lorenzo-Redondo, Anita K. Opdycke, Claudia Hawkins, Robert L. Murphy, Agha Mirza, Madison Conte, Nicholas Gallagher, Chun Huai Luo, Junko Jarrett, Abigail Conte, Ruifeng Zhou, Mireille Farjo, Gloria Rendon, Christopher J. Fields, Leyi Wang, Richard Fredrickson, Melinda E. Baughman, Karen K. Chiu, Hannah Choi, Kevin R. Scardina, Alyssa N. Owens, John Broach, Bruce Barton, Peter Lazar, Matthew L. Robinson, Heba H. Mostafa, Yukari C. Manabe, Andrew Pekosz, David D. McManus, and Christopher B. Brooke. Longitudinal analysis of SARS-CoV-2 vaccine breakthrough infections reveal limited infectious virus shedding and restricted tissue distribution. *Open Forum Infectious Diseases*, page ofac192, Apr 2022.
- [68] Kuo-Chien Tsaoa, Yung-Bin Kuob, Chung-Guei Huang, Shao-Wen Chaue, and Err-Cheng Chan. Performance of rapid-test kits for the detection of the pandemic influenza A/H1N1 virus. *Journal of Virological Methods*, 173:387–389, February 2011.
- [69] Quickvue RSV10 rapid antigen test product specification. [https://www.quidel.com/sites/default/files/product/documents/February 2, 2022.](https://www.quidel.com/sites/default/files/product/documents/February%202022.pdf)
- [70] Andrew Pekosz, Valentin Parvu, Maggie Li, Jeffrey C Andrews, Yukari C Manabe, Salma Kodsi, Devin S Gary, Celine Roger-Dalbert, Jeffry Leitch, and Charles K Cooper. Antigen-based testing but not real-time polymerase chain reaction correlates with severe acute respiratory syndrome coronavirus 2 viral culture. *Clinical Infectious Diseases*, 73(9):e2861–e2866, Nov 2021.
- [71] Emily N. Gallichotte, Kendra M. Quicke, Nicole R. Sexton, Emily Fitzmeyer, Michael C. Young, Ashley J. Janich, Karen Dobos, Kristy L. Pabilonia, Gregory Gahm, Elizabeth J. Carlton, Gregory D. Ebel, and Nicole Ehrhart. Early adoption of longitudinal surveillance for SARS-CoV-2 among staff in long-term care facilities: Prevalence, virologic and sequence analysis. *Microbiology Spectrum*, 9(3):e01003–21, Nov 2021.
- [72] Soha Al Bayat, Jasha Mundodan, Samina Hasnain, Mohamed Sallam, Hayat Khogali, Dina Ali, Saif Alateeg, Mohamed Osama, Aiman Elberdiny, Hamad Al-Romaihi, and Mohammed Hamad J. Al-Thani. Can the cycle threshold (Ct) value of RT-PCR test for SARS CoV2 predict infectivity among close contacts? *Journal of Infection and Public Health*, 14(9):1201–1205, Sep 2021.

Supplemental Figures and Tables

Figure S1: **Optimal use of tests depends on the number of tests available and when they are used.** Testing Effectiveness (TE) of RDT and RT-qPCR with 2 day turnaround time, used x days after exposure using y tests once per day is shown for RSV (orange), influenza type A (pink), and SARS-CoV-2 omicron in experienced hosts (green). Darker colors represent higher TE as indicated. In each row, the testing strategy with highest TE is annotated with a white star. Turnaround times: rapid tests, TAT = 0; RT-qPCR TAT = 2. See Supplementary Table S1 for LODs.

Pathogen	Parameter	Value	Units	Source
Influenza A	Latent period	Unif[0.5,1.5]	Days from exposure	[26, 27]
	Peak time	Unif[1,3]	Days from latent	[26–28]
	Peak VL	Unif[6,8.5]	log ₁₀ cp RNA/mL	[28]
	Clearance time	Unif[2,3]	Days from VL peak	[26–28]
	Infectious threshold	4	log ₁₀ cp RNA/mL	[34]
	High sensitivity LOD	2.95	log ₁₀ cp RNA/mL	[28]
	Low sensitivity LOD	5.38	log ₁₀ cp RNA/mL	[68]
	Percent symptomatic	64	Percent of infections	[26–28]
	Symptom onset time	Unif[-2,0]	Days from VL peak	[34]
Failure rate	5	Percent of tests above LOD	See text	
RSV	Latent period	Unif[2,4]	Days from exposure	[24, 25]
	Peak time	Unif[2,4]	Days from latent	[24]
	Peak VL	Unif[4,8]	log ₁₀ cp RNA/mL	[24, 25]
	Clearance time	Unif[3,6]	Days from VL peak	[24, 25]
	Infectious threshold	2.8	log ₁₀ cp RNA/mL	[25]
	High sensitivity LOD	2.8	log ₁₀ cp RNA/mL	[24]
	Low sensitivity LOD	5	log ₁₀ cp RNA/mL	[69]
	Percent symptomatic	57	Percent of infections	[35, 66]
	Symptom onset time	Unif[-1,1]	Days from VL peak	[62]
Failure rate	5	Percent of tests above LOD	See text	
SARS-CoV-2 omicron strain experienced host	Latent period	Unif[2.5,3.5]	Days from exposure	[12, 29]
	Peak time	Lognormal[1.053,0.688]*	Days from latent	[30]
	Peak VL	Lognormal[1.876,0.181]	40 - Cycle threshold	[30]
	Clearance time	Lognormal[1.704,0.491] [†]	Days from VL peak	[30]
	Infectious threshold	5.5	log ₁₀ cp RNA/mL	[32, 70–72]
	High sensitivity LOD	3	log ₁₀ cp RNA/mL	[29, 30]
	Low sensitivity LOD	6	log ₁₀ cp RNA/mL	[40, 41]
	Percent symptomatic	65	Percent of infections	[30]
	Symptom onset time	Unif[-5,-1]	Days from VL peak	[30, 44, 45]
Failure rate	5	Percent of tests above LOD	[40]	
SARS-CoV-2 founder strain naive host	Latent period	Unif[2.5,3.5]	Days from exposure	[12, 29]
	Peak time	Lognormal[0.873,0.788]*	Days from latent	[16]
	Peak VL	Lognormal[1.999,0.199]	log ₁₀ cp RNA/mL	[16]
	Clearance time	Lognormal[1.953,0.611] [†]	Days from VL peak	[16]
	Infectious threshold	5.5	log ₁₀ cp RNA/mL	[32, 70–72]
	High sensitivity LOD	3	log ₁₀ cp RNA/mL	[30]
	Low sensitivity LOD	5	log ₁₀ cp RNA/mL	[41]
	Percent symptomatic	65	Percent of infections	[29, 30]
	Symptom onset time	Unif[0,3]	Days from VL peak	[29, 63, 64]
Failure rate	5	Percent of tests above LOD	See text	

Table S1: **Summary of viral load, infectiousness, and testing parameters.** For a description of how parameters were extracted from the cited sources, please see Materials and Methods. LOD, limit of detection; VL, viral load; Unif, uniform; * bounded within [0.5, 10]; [†] bounded within [0.5, 25].

Supplementary Text: Imperfect Isolation Behaviors

To include imperfect post-diagnosis isolation behaviors, we consider a behavior change function $B(\tau)$, one's relative infectiousness at time since diagnosis τ . For instance, perfect isolation upon diagnosis would be modeled as $B(\tau) = 0$, while a one-week partial isolation might be modeled as $B(\tau) = 0.5$ for $0 \leq \tau \leq 7$, and $B(\tau) = 1$ for $\tau > 7$. The individual reproduction number can thus be written as the sum of the total infectiousness before and after diagnosis,

$$\nu_{\text{testing}}(t_{\text{Dx}}) = \int_0^{t_{\text{Dx}}} \beta(t) dt + \int_{t_{\text{Dx}}}^{\infty} B(t - t_{\text{Dx}})\beta(t) dt . \quad (\text{S1})$$

Simplifying yields

$$\bar{\nu}_{\text{testing}} = \nu_0 - \int_0^{\infty} \int_0^t \beta(t) [1 - B(t - t_{\text{Dx}})] f(t_{\text{Dx}}) dt_{\text{Dx}} dt . \quad (\text{S2})$$

This equation offers a helpful term-by-term interpretation: diagnosis decreases total infectiousness from its baseline of ν_0 by an amount that depends on (i) the probability distribution of diagnosis times $f(t_{\text{Dx}})$ and (ii) the quality of isolation after said diagnosis $B(\tau)$, weighted by (iii) the infectiousness $\beta(t)$ at the time of isolation and thereafter. Under a specified isolation behavior $B(\tau)$, TE is computed as

$$TE = p \int_0^{\infty} \mathbb{E} \left[\beta(t) \left(\int_0^t [1 - B(t - t_{\text{Dx}})] f(t_{\text{Dx}}) dt_{\text{Dx}} \right) \right] dt / \int_0^{\infty} \mathbb{E} [\beta(t)] dt . \quad (\text{S3})$$

Thus, more complex post-diagnosis behaviors may be easily modeled, but such scenarios were not explored numerically in the main text.

Supplementary Text: Test to Exit Strategies

Test-to-exit (TTE) is a strategy designed to maximize the effectiveness of post-diagnosis isolation while minimizing the number of days spent in isolation by requiring one or more negative test(s) before exiting isolation. While various formulations of TTE may exist, here we analyze a simple version in which individuals wait w days after receiving a diagnosis and then begin testing at a rate \bar{A} tests per day, with a per-test failure rate of ϕ and a test turnaround time of TAT. We assume that compliance with TTE is $c = 1$ due to individuals' expected desire to leave isolation.

Mirroring Eq. (S1), the expected infectiousness under a test-to-exit program, assuming perfect isolation between the time of diagnosis t_{Dx} and the time of isolation exit t_{exit} , is given by

$$\nu_{\text{testing}}(t_{\text{Dx}}, t_{\text{exit}}) = \int_0^{t_{\text{Dx}}} \beta(t) dt + \int_{t_{\text{exit}}}^{\infty} \beta(t) dt . \quad (\text{S4})$$

We define the PDF and CDF of t_{exit} as g and G , respectively, allowing us to rewrite the previous equation as

$$\bar{\nu}_{\text{testing}} = \nu_0 - \int_0^{\infty} \beta(t) F(t) dt + \int_0^{\infty} \beta(t) \int_0^t G(t, t_{\text{Dx}}) f(t_{\text{Dx}}) dt_{\text{Dx}} dt . \quad (\text{S5})$$

This expression takes on the interpretable form of total infectiousness in the absence of testing ν_0 , minus post-diagnosis infectiousness prevented due to perfect and indefinite isolation, plus any residual infectiousness realized by an exit from isolation.

To model post-isolation exit testing, we assume that one waits w days before testing at a rate \bar{A} using a test with turnaround time TAT and failure rate ϕ . Under these conditions, $n(t) = \bar{A}(t - t_{Dx} - \text{TAT} - w)$ represents the expected cumulative number of scheduled tests with the potential to return an exit-inducing result by time t , with $\bar{n}(t) = n(t) \bmod 1$. The distribution for t_{exit} is then given by the rather cumbersome

$$G(t, t_{Dx}) = \begin{cases} 0 & t \leq t_{Dx} + w + \text{TAT} \\ \psi_1(t) & t_{Dx} + w + \text{TAT} \leq t \leq t_{max} \\ \psi_2(t) & t \geq t_{max} \end{cases} \quad (\text{S6})$$

where the function

$$\psi_1(t) = 1 - \left[(1 - \bar{n}(t))(1 - \phi)^{n(t) - n(\bar{t})} + n(\bar{t})(1 - \phi)^{n(t) - \bar{n}(t) + 1} \right] \quad (\text{S7})$$

represents the cumulative probability that one receives a negative test due to a false negative (i.e., a test failure when above that test's limit of detection), and where

$$\psi_2(t) = \min \left\{ 1, \bar{A} [1 - \psi_1(t_{max})][t - t_{max}] + \psi_1(t_{max}) \right\} \quad (\text{S8})$$

captures the rapid approach of G toward guaranteed exit from isolation after one is no longer detectable. The quantity $t_{max} = \max [t_u + \text{TAT}, t_{Dx} + w + \text{TAT}]$ represents the latest possible time at which a person testing to exit could receive a positive test. The corresponding PDF is

$$g(t, t_{Dx}) = \begin{cases} 0 & t \leq t_{Dx} + w + \text{TAT} \\ \bar{A}\phi(1 - \phi)^{n(t) - \bar{n}(t)} & t_{Dx} + w + \text{TAT} \leq t \leq t_u + \text{TAT} \\ \bar{A} [1 - \psi_1(t_{max})] & t_u + \text{TAT} \leq t \leq t_u + \text{TAT} + 1/\bar{A} \\ 0 & t \geq t_u + \text{TAT} + 1/\bar{A}. \end{cases} \quad (\text{S9})$$

Under the above TTE assumptions, the typical number of days spent in isolation may be computed as the expected difference between the t_{exit} and t_{Dx} distributions. One may also update \bar{q}_{Dx} in computing test consumption (Materials and Methods) to include the additional tests consumed while testing to exit,

$$\bar{q}_{\text{TTE}} = 1 + \int_0^\infty \int_{t_{Dx} + w}^\infty \left(\left| \int_{t_{Dx} + w}^{t_{\text{exit}} - \text{TAT}} \bar{A} dt \right| + \left| \int_{t_{\text{exit}} - \text{TAT}}^{t_{\text{exit}}} \bar{A} dt \right| \right) g(t_{\text{exit}}, t_{Dx}) f(t_{Dx}) dt_{\text{exit}} dt_{Dx} . \quad (\text{S10})$$